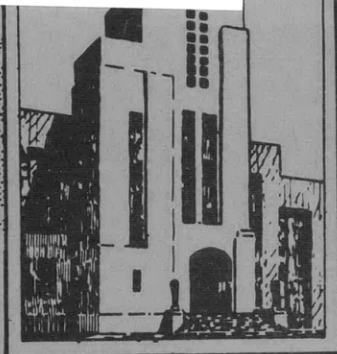


V393  
.R46

~~Handwritten scribble~~

~~Handwritten scribble~~  
R 81059

MIT LIBRARIES



DEPARTMENT OF THE NAVY  
DAVID TAYLOR MODEL BASIN



HYDROMECHANICS

NATURAL MODES AND FREQUENCIES OF VERTICAL VIBRATION  
OF A BEAM WITH AN ATTACHED SPRUNG MASS



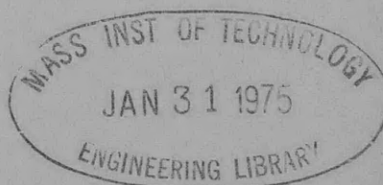
by

AERODYNAMICS

Ralph C. Leibowitz



STRUCTURAL  
MECHANICS

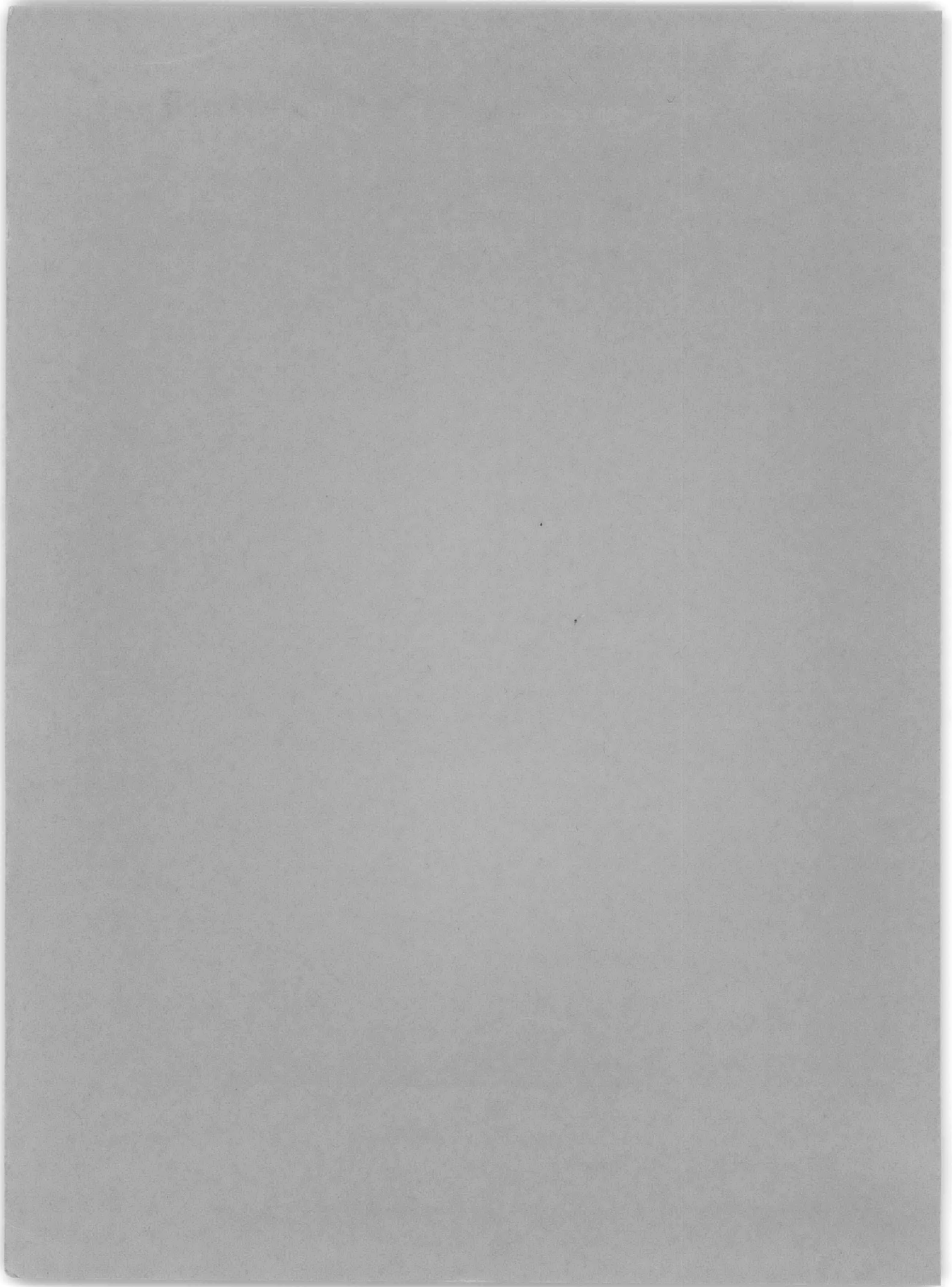


STRUCTURAL MECHANICS LABORATORY  
RESEARCH AND DEVELOPMENT REPORT

APPLIED  
MATHEMATICS

September 1958

Report 1215



**NATURAL MODES AND FREQUENCIES OF VERTICAL VIBRATION  
OF A BEAM WITH AN ATTACHED SPRUNG MASS**

**by**

**•Ralph C. Leibowitz**

**September 1958**

**Report 1215  
NS 712-100**

## TABLE OF CONTENTS

	Page
ABSTRACT .....	1
1. INTRODUCTION .....	1
2. EFFECTS OF SPRUNG MASS ON FREQUENCIES .....	2
2.1. Qualitative Aspects of Sprung-Mass Theory .....	2
2.2. Analytical Method of Solution for Natural Frequencies of Uniform Beam with Sprung Mass Attached .....	4
2.3. Natural Frequencies of Uniform Beam with Sprung Mass Attached as Determined by TMB Network Analyzer .....	5
2.4. Natural Frequencies of Nonuniform Beam with Sprung Mass Attached as Determined by TMB Network Analyzer .....	7
3. EFFECTS OF SPRUNG MASS ON MODE SHAPES .....	9
4. APPLICATION OF SPRUNG-MASS THEORY TO SS GOPHER MARINER .....	19
5. CONCLUSIONS .....	19
6. ACKNOWLEDGMENTS .....	20
APPENDIX A – RELATIONSHIP BETWEEN FORCE $F_p$ ACTING ON BEAM AND NATURAL FREQUENCIES OF COMBINED SPRUNG-MASS SYSTEM .....	21
APPENDIX B – DERIVATION OF RESPONSE RATIO $y_p/F_p$ OF AN UNDAMPED FREE-FREE UNIFORM BEAM WITHOUT SHEAR AND WITH A SPRUNG MASS ATTACHED .....	23
APPENDIX C – ELECTRICAL ANALOG OF A UNIFORM BEAM-SPRUNG- MASS SYSTEM .....	29
APPENDIX D – ACCURACY OF FREQUENCY CORRESPONDING TO ADDED MODE FOR UNDAMPED FREE-FREE UNIFORM BEAM WITH SPRUNG MASS ATTACHED .....	33
APPENDIX E – ELECTRICAL ANALOG OF NONUNIFORM BEAM-SPRUNG- MASS SYSTEM .....	35
APPENDIX F – GRAPHICAL DETERMINATION OF ADDED MODE FREQUENCY OF NONUNIFORM BEAM.....	37
REFERENCES .....	38

## LIST OF ILLUSTRATIONS AND TABLES

	Page
Figure 1 – Beam with Attached Spring-Mass System .....	3
Figure 2 – Response Ratio $y_p/F_p$ for a Beam and a Sprung Mass as a Function of Frequency .....	3
Figure 3 – Modes of Vertical Vibration of GOPHER MARINER Determined by TMB Network Analyzer and UNIVAC .....	10
Figure 4 – Modes of Vertical Vibration of GOPHER MARINER with and without a 10-Percent Sprung Mass Attached at Station 10 Determined by TMB Network Analyzer .....	13
Figure 5 – Modes of Vertical Vibration of GOPHER MARINER with and without a 50-Percent Sprung Mass Attached at Station 10 Determined by TMB Network Analyzer .....	17
Figure 6 – Vertical-Amplitude Profiles of GOPHER MARINER Experimentally Obtained for Light-Loading Condition at Vibration Generator Speeds of 165, 237, 285, 365, and 485 RPM .....	18
Figure 7 – Coordinate System with Origin at (0, 0) .....	24
Figure 8 – Coordinate System with Origin at ( $l$ , 0) .....	24
Figure 9 – Sign Convention for Moments and Forces Acting on Beam .....	26
Figure 10 – Analog of Uniform GOPHER MARINER Beam with Bending Flexibility only and without Sprung Mass .....	29
Figure 11 – Sprung-Mass System .....	30
Figure 12 – Sprung-Mass Mobility Analog Added at Station $n = 10$ , to 20-Section Analog Shown in Figure 10 .....	31
Figure 13 – Response Ratios for a Beam and a Sprung Mass as a Function of Frequency .....	33
Figure 14 – Analog of 20-Section Nonuniform GOPHER MARINER Beam with Attached Sprung Mass with Bending and Shearing Flexibility .....	36
Table 1 – Natural Frequencies of Uniform GOPHER MARINER Beam with Bending Flexibility Only .....	6
Table 2 – Natural Frequencies of Undamped Free-Free Nonuniform Beam with Bending and Shearing Flexibility as Obtained by TMB Network Analyzer .....	8
Table 3 – Data for Analog of 20-Section Nonuniform GOPHER MARINER Beam with Bending and Shearing Flexibility .....	35

## NOTATION

$b$	Distance along beam from origin to point $P$
$(EI)_n$	Flexural rigidity of beam at station $n$
$F_p$	Force acting on beam at point $P$
$-F_p$	Force acting on sprung mass
$f_n$	Natural mechanical frequencies of free vibration of free-free beam in cpm, $n = 1, 2, \dots$
$f'_n$	Natural mechanical frequencies of free vibration of combined system
$f'_{na}$	Additional natural mechanical frequency of a beam-sprung-mass system in cpm
$f_0$	Natural mechanical frequency of free vibration of mass-spring system alone in cpm
$I$	Sectional area moment of inertia
$K$	Spring constant
$k$	$\left(\frac{\mu\omega^2}{EI}\right)^{1/4}$
$(KAG)_n$	Shear rigidity of beam at station $n$
$l$	Length of beam
$M_n$	Bending moment acting on beam at station $n$
$m$	Sprung mass
$m_e$	Effective mass (equivalent of sprung mass, see Appendix A)
$m_n$	Mass of beam element lumped at station $n$
$m_n^s$	Sprung mass at station $n$
$t$	Time
$V_n$	Shearing force acting on beam; see Figure 9 for sign convention
$x$	Longitudinal distance from left end of beam
$x'$	Longitudinal distance from right end of beam to point $x$ ; see Figure 8
$y$	Lateral deflection of beam
$y_m$	Displacement of sprung mass in $y$ -direction
$y_n^s$	Displacement of sprung mass in $y$ -direction at station $n$
$\dot{y}_n^s$	Velocity of sprung mass at station $n$
$\ddot{y}_n^s$	Acceleration of sprung mass at station $n$
$y_p$	Displacement of beam in $y$ -direction at point $P$ on beam

$\alpha$	$\frac{\left(\frac{\Delta x}{EI}\right)'}{\left(\frac{\Delta x}{EI}\right)}$
$\beta$	$\frac{\left(\frac{\Delta x}{KAG}\right)'}{\left(\frac{\Delta x}{KAG}\right)}$
$\Delta x$	Length of element, $\frac{l}{20}$
$\epsilon_1$	Percent difference between exact theoretical values and TMB network analyzer values of natural frequencies of a beam without a sprung mass attached
$\epsilon_2$	Percent difference between exact theoretical values and TMB network analyzer values of natural frequencies of a beam with a sprung mass attached
$\lambda$	$\frac{m_n'}{m_n}$
$\mu$	Mass per unit length
$\mu \Delta x$	Mass of beam element of length $\Delta x$ (including its virtual mass)
$\nu$	$\frac{t}{t'}$
$\tau$	$\frac{\Delta x}{(\Delta x)'}$
$\omega$	Forcing frequency on beam
$\omega_a$	Antiresonance frequency
$\omega_n$	Natural circular frequency of free vibration of free-free beam
$\omega_n'$	Natural circular frequency of free vibration of combined system
$\omega_0'$	Natural circular frequency of free vibration of mass-spring system alone
'	With the exception of frequency and $x'$ electrical quantities analogous to mechanical quantities are denoted by a primed exponent such as $V_n'$ corresponding to $V_n$





## ABSTRACT

A study was made of the vibration characteristics of a beam with an attached sprung mass. The purpose was to explore the possibility of a more adequate representation of a ship hull as a mass-elastic system subject to vibration. Analytical and electrical-analog methods are devised to determine the natural frequencies and mode shapes of a beam-sprung-mass system. These methods are shown to give results that are reasonably accurate.

## 1. INTRODUCTION

On certain classes of ships, flexibly mounted masses such as machinery, rudders, cargo, and superstructures affect hull vibrations.<sup>1,2,3\*</sup> It is therefore of value to investigate the characteristics of a beam with an attached sprung mass, as a step toward achieving a more adequate representation of a ship hull as a mass-elastic system subject to vibration.

The unusual mode shapes observed on SS GOPHER MARINER (Reference 1, Figure 19) led to the consideration of local flexibility or the sprung-mass effect as a possible explanation of the "unbeamlike" patterns. A study of the qualitative effects of a single sprung mass on the vibration of a beam is given in Reference 4. An unsuccessful attempt to code the problem of the nonuniform beam with sprung masses for solution on the UNIVAC computer led to the present work, which is based on use of the David Taylor Model Basin Network Analyzer.\*\*

This report discusses the effect of a flexibly attached mass on the natural frequencies and modes of beam vibration. The specific objectives of the report are:

1. To substantiate and extend, by mathematical and electrical-analog methods, the qualitative theory of the vibration characteristics of a beam with an attached sprung mass, as advanced by Kennard.<sup>4</sup> An analytical expression and electrical-analog methods are devised to determine the natural frequencies of a *uniform* beam-sprung-mass system. The natural frequencies obtained therefrom are shown to agree with the qualitative predictions of Kennard. In addition, the effects of a sprung mass on the natural frequencies and mode shapes of the *nonuniform* beam to which it is attached are shown by means of the electrical analog.
2. To determine the accuracy with which the natural frequencies of a beam-sprung-mass system can be obtained with the TMB network analyzer by comparing the theoretical and analog frequencies of a uniform beam.
3. To determine the accuracy with which the mode shapes of a beam-sprung-mass system can be obtained with the TMB network analyzer.
4. To explain the unusual mode shapes observed on the SS GOPHER MARINER.<sup>1</sup> It is

---

\*References are listed on page 38.

\*\*The sprung-mass problem has recently been successfully coded for solution on the UNIVAC.

shown that the local flexibility or sprung-mass effect could cause the “unbeamlike” patterns obtained.

The report treats, in sequence, the effects of a sprung mass on the frequencies and on the modes of vibration of the beam to which it is attached. General conclusions are given with regard to these effects.

## 2. EFFECTS OF SPRUNG MASS ON FREQUENCIES

### 2.1. QUALITATIVE ASPECTS OF SPRUNG-MASS THEORY

The effect of local elasticities and masses on the natural frequencies of a ship can be studied *qualitatively* by considering the idealized sprung mass attached to the free-free beam. The effects of a sprung mass are discussed in Reference 4. However, for completeness of this report, some relevant qualitative results of a beam-sprung-mass system will be given here.

Consider a mass  $m$  which is spring-mounted at a point  $P$ , as shown in Figure 1. Let  $K$  denote the spring constant.

The oscillatory internal forces acting on the beam at  $P$  and on the mass and the displacements during a free vibration of the combined system are shown in Figure 1. The arrows indicate instantaneous directions. Note that, alternatively, the force  $F_p$  may be considered the force maintaining a forced vibration of the beam.

The response ratio is plotted against  $\omega$ , the frequency of a sinusoidal applied force,<sup>4</sup> for both the free-free beam and sprung mass alone in Figure 2. In Figure 2 the curve  $y_p/F_p$  for the sprung mass alone is drawn for four possible alternative positions labeled A, B, C, and D.

The intersections of the two types of curves in Figure 2 give the natural frequencies of of the *combined* beam-sprung-mass system. Inspection shows that all the natural frequencies  $\omega_n$  which exist for the beam alone are “repelled” by the frequency  $\omega_0 = \sqrt{\frac{K}{m}}$ , the natural circular frequency for free vibration of the mass-spring system alone when the point  $P$  is fixed. Those frequencies for which  $\omega_n < \omega_0$  are replaced by lower frequencies for the system; those for which  $\omega_n > \omega_0$  are replaced by higher frequencies. Also a new mode of vibration of the combined system is added because of the additional degree of freedom corresponding to the added sprung mass. The new frequency will also lie between the two natural frequencies of the beam alone which lie adjacent to the frequency  $\omega_0$  of the sprung mass. If  $\omega_0$  happens to coincide with an antiresonance frequency  $\omega_a$ , then the added natural frequency is  $\omega_a$ . If  $\omega_0$  coincides with a natural frequency  $\omega_n$  of the beam, then the added sprung mass will give rise to two natural frequencies of the combined systems which lie on each side of  $\omega_n$ .

It is interesting to observe that for a given  $\omega_0$  and varied mass, a family of curves passes through the point  $\omega = \omega_0$ . The smaller the sprung mass, the steeper the curve. For a given beam the added natural frequency corresponding to a sprung mass will deviate less from  $\omega_0$  for the smaller mass; the larger the sprung mass, the larger the deviation from  $\omega_0$ .

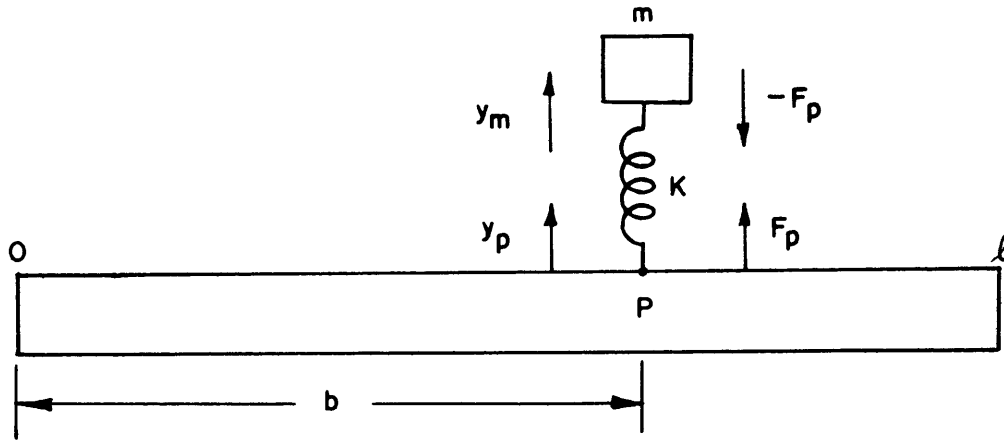


Figure 1 – Beam with Attached Spring-Mass System

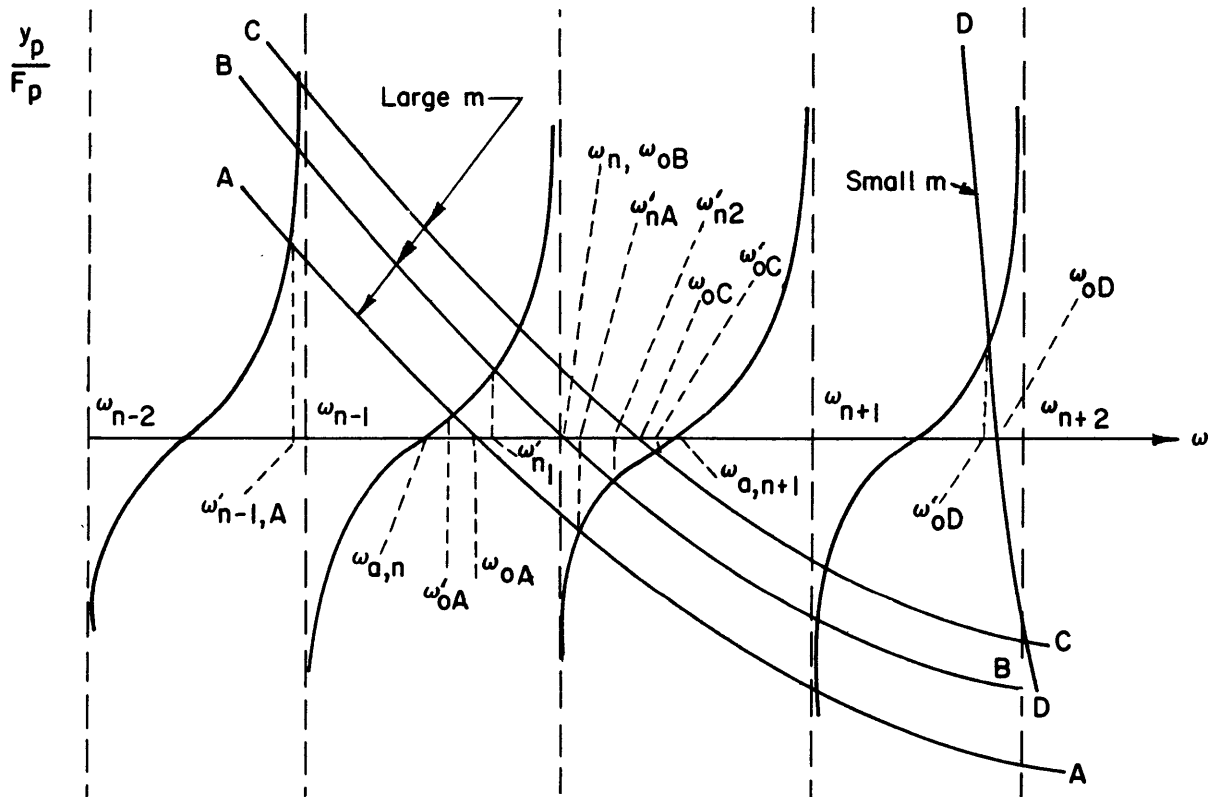


Figure 2 – Response Ratio  $y_p/F_p$  for a Beam and a Sprung Mass as a Function of Frequency

$\omega_n; \omega_{n-1}; \omega_{n-2}; \omega_{n+1}; \omega_{n+2}$  and  $\omega_{a,n}; \omega_{a,n+1}$  are the circular resonance and antiresonance frequencies of the beam alone.

$\omega_{0A}; \omega_{0B}; \omega_{0C}; \omega_{0D}$  are possible natural circular frequencies of the mass-spring system.

Primed symbols indicate the frequencies resulting when the mass-spring system is attached to the beam. For curve B,  $\omega_n$  and  $\omega_{0B}$  coincide and the altered values are designated  $\omega'_{n1}$  and  $\omega'_{n2}$ .

For a given location of the sprung mass on the beam and a given  $\omega_0$ , it is the magnitude of the sprung mass alone which determines the degree to which the original natural frequencies of the free-free beam are repelled.

It should also be noted that the *shape* of the curves of  $\frac{y_p}{F_p}$  versus  $\omega$  for the beam alone is determined both by the physical parameters of the beam and by the location  $P$  of the applied force (the sprung-mass location).

## 2.2. ANALYTICAL METHOD OF SOLUTION FOR NATURAL FREQUENCIES OF UNIFORM BEAM WITH SPRUNG MASS ATTACHED

The free vibration of a free-free *uniform* beam with an attached sprung mass will be treated on the assumptions that the beam has bending flexibility only and that the damping forces are negligible. These assumptions permit an analytical determination of the natural frequencies of the system for comparison with the values determined with the TMB network analyzer as described in Section 2.3.

It is shown in Appendix A that the response ratio  $\frac{y_p}{F_p}$  at point  $P$  of the beam shown in Figure 1 is

$$\frac{y_p}{F_p} = \frac{\omega_0^2 - \omega^2}{m\omega_0^2 \omega^2} \quad [1]$$

where  $\omega_0 = \sqrt{\frac{K}{m}}$  is the natural circular frequency for free vibration of the mass-spring system alone when the point  $P$  is fixed and  $\omega$  is the frequency of the force  $F_p$  applied to the beam.

For the case of an undamped, free-free, uniform beam with bending flexibility only, the response ratio  $\frac{y_p}{F_p}$  of the beam at point  $P$  is also (see Appendix B)

$$\frac{y_p}{F_p} = \frac{1}{2k^3 EI} \frac{\left[ \begin{array}{l} \cos k(l-b) \sinh k(l-b) - \sin k(l-b) \cosh k(l-b) \\ + \cos k(l-b) \cos kb \sinh kl - \sin kl \cosh kb \cosh k(l-b) \\ + \cos kb \sinh kb - \sin kb \cosh kb \end{array} \right]}{1 - \cos kl \cosh kl} \quad [2]$$

where  $k = \left( \frac{\mu \omega^2}{EI} \right)^{1/4}$ , and

$\mu$  is the mass per unit length,

$E$  is Young's modulus,

$I$  is the sectional area moment of inertia,

$l$  is the length of the beam, and

$b$  is the distance along the beam from the origin to the point  $P$  in Figure 1.

Equating the right members of Equations [1] and [2] gives

$$\frac{\omega_0^2 - \omega^2}{m\omega_0^2 \omega^2} = \frac{1}{2k^3 EI} \frac{\left[ \begin{array}{l} \cos k(l-b) \sinh k(l-b) - \sin k(l-b) \cosh k(l-b) \\ + \cos k(l-b) \cos kb \sinh kl - \sin kl \cosh kb \cosh k(l-b) \\ + \cos kb \sinh kb - \sin kb \cosh kb \end{array} \right]}{1 - \cos kl \cosh kl} \quad [3]$$

Equation [3] may be solved for  $\omega$  by trial and error for particular values of  $\omega_0$ ,  $m$ ,  $\mu$ ,  $E$ ,  $I$ ,  $l$ ,  $b$ . The values of  $\omega_n'$  thus found are the natural frequencies of the combined beam-sprung-mass systems. This numerical method is tedious. It is easier to determine the natural frequencies and modes of vibration by use of the TMB network analyzer. However, the equation has been solved for a particular uniform beam in order to obtain a comparison between the exact solution and the analog results. The beam parameters and the results of the computations are given in the next section.

### 2.3. NATURAL FREQUENCIES OF UNIFORM BEAM WITH SPRUNG MASS ATTACHED AS DETERMINED BY TMB NETWORK ANALYZER

The electrical circuit which represents lateral vibrations of a beam is given in Reference 5. This circuit has been slightly modified to take account of the added sprung mass; see Appendix C. For the calculations given in this report the beam was divided into 20 sections, each of length  $\Delta x$ , and electrical measurements of the voltages which represent the vibratory motions were made at 21 points along the beam.

Both *analytical* and *analog* procedures were applied to a *uniform* beam, every section of which has the same mass per unit length and bending stiffness  $EI$  as the midship section of SS GOPHER MARINER.<sup>1</sup> The physical data are:

$$\begin{aligned} EI &= 1.50 \times 10^{10} \text{ ton-ft}^2 \\ l &= 525 \text{ ft} \\ \Delta x &= l/20 = 26.25 \text{ ft} \\ \Delta x/EI &= 1.75 \times 10^{-9} \text{ (ton-ft)}^{-1} \\ b &= l/2 = 262.5 \text{ ft} \\ \mu &= 3.49 \text{ ton-sec}^2/\text{ft}^2 \\ \mu \Delta x &= 91.6 \text{ ton-sec}^2/\text{ft} \end{aligned}$$

The sprung mass is taken as 50 percent of the effective ship mass\* in a length  $\Delta x = l/20$  or as 45.81 ton-sec<sup>2</sup>/ft. Assume the natural frequency  $\omega_0$  of the mass-spring system

---

\*The effective ship mass is the mass of the hull plus its virtual mass.

TABLE 1

Natural Frequencies of Uniform GOPHER MARINER Beam  
with Bending Flexibility Only

TMB network analyzer results are for a beam subdivided into 20 sections.

Without Sprung Mass				With Sprung Mass**				
Mode	Frequency, cpm		$\epsilon_1^{***}$ Percent	Mode	Frequency, cpm		$\epsilon_2^{***}$ Percent	$\epsilon_2 - \epsilon_1$ Percent
	Free-Free Bar Equation	TMB Network Analyzer			Equation [3]	TMB Network Analyzer		
1	2	3	4	5	6	7	8	9
1	50.85	51.6	-1.485	1	50	50.4	-0.99	+0.495
2	140	136.2	+2.82	2	140	136.2	+2.69	-0.13
3	274.5	264.6	+3.74	3	263	252	+4.16	+0.42
				3a*	392.5	389.4	+0.88	
4	454	418.8	+7.76	4	455	419.4	+7.65	-0.12
5	678.5	601.8	+11.6	5	685	612.6	+10.6	-1.0
6	953.5	810.6	+14.9	6		810.6		

\*The frequency corresponding to Mode 3a is the additional natural mechanical frequency of the beam-sprung-mass system.

\*\*A sprung mass of 45.81 ton-sec<sup>2</sup>/ft was attached at Station 10 on the beam. The frequency  $f_0$  was 370 cpm.

\*\*\*  $\epsilon_1$  (without sprung mass) =  $\frac{[f_{n \text{ Free-Free Bar}} - f_{n \text{ Network Analyzer}}]}{f_{n \text{ Free-Free Bar}}} \times 100$  percent

\*\*\*  $\epsilon_2$  (with sprung mass) =  $\frac{[f'_{n \text{ Equation [3]}} - f'_{n \text{ Network Analyzer}}]}{f'_{n \text{ Equation [3]}}} \times 100$  percent

alone to fall between the frequencies of the third and fourth modes of the free beam. Arbitrarily choose  $\omega_0 = 7.28 \omega_1$ , where  $\omega_1$  is the fundamental frequency of the free-free beam<sup>6</sup>:

$$\omega_1 = \frac{(4.73)^2}{l^2} \sqrt{\frac{EI}{\mu}} \frac{\text{rad}}{\text{sec}} \quad [4]$$

since  $\omega_1 = 5.32$  rad/sec,  
 $\omega_0 = 38.73$  rad/sec, and  
 $K = \omega_0^2 m = 68,715$  ton/ft.

The natural frequencies  $\omega_n$  of the free-free "classical" beam<sup>7</sup> fall in the ratios 1: 2.756; 5.405: 8.93; 13.34: 18.74. The values of  $f_n$  corresponding to the exact solutions for the free-free beam are given in Column 2 of Table 1, and the corresponding values obtained with the network analyzer are given in Column 3. The values of  $f'_n$  of the beam-sprung-mass system computed from Equation [3] are given in Column 6, and the corresponding values obtained with the network analyzer are given in Column 7.

The errors shown in Table 1 are largely inherent in the lumping procedure (i.e., lumped electrical parameters are used to represent a continuous physical system) and in the imperfect components used in the network analyzer, and are not random. Since the analog representation used for the free-free beam was also incorporated in the analog of the beam-sprung-mass system, it would be expected that the errors  $\epsilon_2$  and  $\epsilon_1$ , defined in Table 1, would be nearly equal. The small values of  $\epsilon_2 - \epsilon_1$  verify this prediction, and suggest that the analyzer indicates fairly accurately the effect of sprung masses on the natural frequencies of the beam.

The measured and theoretical values of the new frequency  $f'_{3a}$  agree within 0.88 percent, as shown in Table 1. This unusually good accuracy is explained in Appendix D.

In any mode for which  $f_n < f_0$  (i.e.,  $n = 1, 2, 3$  here) the frequency of the beam with sprung mass is lower than the frequency of the beam without sprung mass. In any mode for which  $f_n > f_0$  (i.e.,  $n = 4, 5$ ) the frequency of the beam with sprung mass is higher than the frequency of the beam without sprung mass. These results are in agreement with Reference 4.

A new frequency is added for the sprung-mass system because of the additional degree of freedom introduced by the added sprung mass.

Since the sprung mass is relatively large, the added mode frequency  $f'_{3a}$  does not lie very close to  $f_0$  (as  $m$  grows smaller  $f'_{3a} \rightarrow f_0$ ).<sup>4</sup> These observations are in accordance with the theory as discussed in Section 2.1.

## 2.4 NATURAL FREQUENCIES OF NONUNIFORM BEAM WITH SPRUNG MASS ATTACHED AS DETERMINED BY TMB NETWORK ANALYZER

The natural frequencies of a nonuniform beam (representing GOPHER MARINER) with an attached sprung mass will now be determined. Both flexural and shear rigidity as well as nonuniform mass distribution are considered. Damping forces are considered to be negligible. The physical and electrical parameters defining the GOPHER MARINER are given in Appendix E. The mass distribution used corresponds to the light ship condition.<sup>1</sup>

The 20-section analog of the beam with and without an attached sprung mass was set up on the TMB network analyzer in accordance with the circuit shown in Figure 14 of Appendix E. Sprung masses equal to 10 percent and 50 percent of the total mass lumped at Station 10 of the original nonuniform beam (without sprung mass) were used to demonstrate their effects on the beam. For each sprung mass,  $f_0$  was taken as 234 cpm, which is equal to the natural frequency of the free-free GOPHER MARINER beam in the third mode. Table 2 gives

TABLE 2

Natural Frequencies of Undamped Free-Free Nonuniform Beam  
with Bending and Shearing Flexibility as  
Obtained by TMB Network Analyzer

Measured electrical frequencies have been converted to cycles per minute (mechanical).

Mode	Frequency without Sprung Mass cpm	Mode	Frequency with 10-Percent Sprung Mass cpm	Frequency with 50-Percent Sprung Mass cpm
1	73	1	78	78
2	154.2	2	154.2	154.2
3	234.0	3a	227.4	209.4
		3b	259.8	268.2
4	320.4	4	321.6	325.2
5	400.2	5	404.4	420.0
6	478.8			

the natural frequencies of the several beam systems. Examination of Table 2 shows that the introduction of the sprung mass yields results which agree with the theory discussed in Section 2.1. In particular, it may be observed that the original beam frequency  $f_3$  is replaced by two new frequencies,  $f'_{3a}$  and  $f'_{3b}$ , either of which can be regarded as the new one since  $f_0$  equals  $f_3$ .

A graphical method of determining, with reasonable accuracy, the added mode frequency of a nonuniform or uniform beam with shear and bending flexibility is given in Appendix F.

It seems reasonable to assume that analog results for the natural frequencies of a uniform and nonuniform beam-sprung-mass system with shear and bending flexibility will be subject to errors of the same order of magnitude, provided that the nonuniformity is not too large. The natural frequencies of a uniform beam with shear and bending flexibility can be computed<sup>8</sup> and compared with analog computations in order to determine the errors in the latter.

For larger nonuniformity the mode frequencies obtained with a digital computer such as the UNIVAC for a beam comprised of 40 sections may be regarded as a standard to determine analog errors.

By inference, the TMB network analyzer may be used also to determine the effect of many sprung masses upon the natural frequencies and mode shapes of a free-free nonuniform beam with shear and bending flexibility, rotary inertia, and damping. The system parameters may be readily changed on the analyzer, and the effects of these changes can be explored rapidly.



### 3. EFFECTS OF SPRUNG MASS ON MODE SHAPES

The quantitative effects of a sprung mass upon the mode *shapes* of a beam, which have been unknown so far, can be determined by use of electrical-analog methods.

Consider again the *nonuniform* beam (representing GOPHER MARINER) discussed in Section 2.4. The mode shapes of the beam obtained on the TMB network analyzer are compared with the corresponding mode shapes determined by the UNIVAC as shown in Figure 3. The UNIVAC solution is considered accurate. The accuracy and the smoothness of the analog mode *shapes* are evident. The greatest deviations of the analog results occur in the highest modes.

It seems reasonable to assume that analog results for the mode *shapes* of a nonuniform beam with or without an attached sprung mass will be subject to errors of the same order of magnitude.

The natural frequencies and normal modes of vibration of the nonuniform beam with and without an attached sprung mass, determined on the TMB network analyzer, are given in Figures 4 and 5. The sprung masses are equal to 10 percent and 50 percent of the mass lumped at Station 10 of the original beams (without sprung mass). Note that, for the beam with the 50-percent sprung mass, the natural frequencies  $f_4'$  and  $f_5'$  were measured although the corresponding mode *shapes* were not determined; see Table 2.

Figures 4 and 5 also show two mode *shapes* with the same number of nodes for the beam-sprung-mass system. *This is contrary to the behavior of beams.*

Inspection of the figures shows too that for the beam-sprung-mass system the mode with a frequency adjacent to and greater than  $f_0$  changes curvature rapidly, i.e., dips, at Station 10 where the sprung mass is attached and the distance between the nodes adjacent to Station 10 lengthens. The greater the sprung mass, the greater the dip. On the other hand, the mode with the frequency adjacent to but less than  $f_0$  has a somewhat sharper peak at Station 10, and the distance between the nodes adjacent to Station 10 diminishes. The greater the sprung mass, the greater this effect.

These modifications to the beamlike mode *shapes* are caused by the phase relationships between the sprung mass and the beam proper. For mode frequencies greater than  $f_0$ , the sprung mass exerts a force which is out of phase with the beam displacement at its point of attachment (i.e., when  $y_p$  is positive, the spring is in compression). For mode frequencies lower than  $f_0$ , the sprung mass exerts a force which is in phase with the beam displacement at its point of attachment (i.e., when  $y_p$  is positive, the spring is in tension). The mathematical relationship between the force acting on the beam at Station 10 and the natural frequencies of the combined beam-sprung-mass system is derived in Appendix A. This force tends to cause the original mode of the beam (without sprung mass), whose resonance frequency falls between the same antiresonance frequencies as  $f_0$ , to be replaced by two mode patterns of the beam-sprung-mass system which have the same number of nodes. The modification of the beamlike modes caused by this force is greatest for those modes which have natural frequencies nearest to  $f_0$ .

Figure 3 – Modes of Vertical Vibration of GOPHER MARINER Determined by TMB Network Analyzer and UNIVAC

The displacement was 18,674 tons corresponding to a condition of light load.

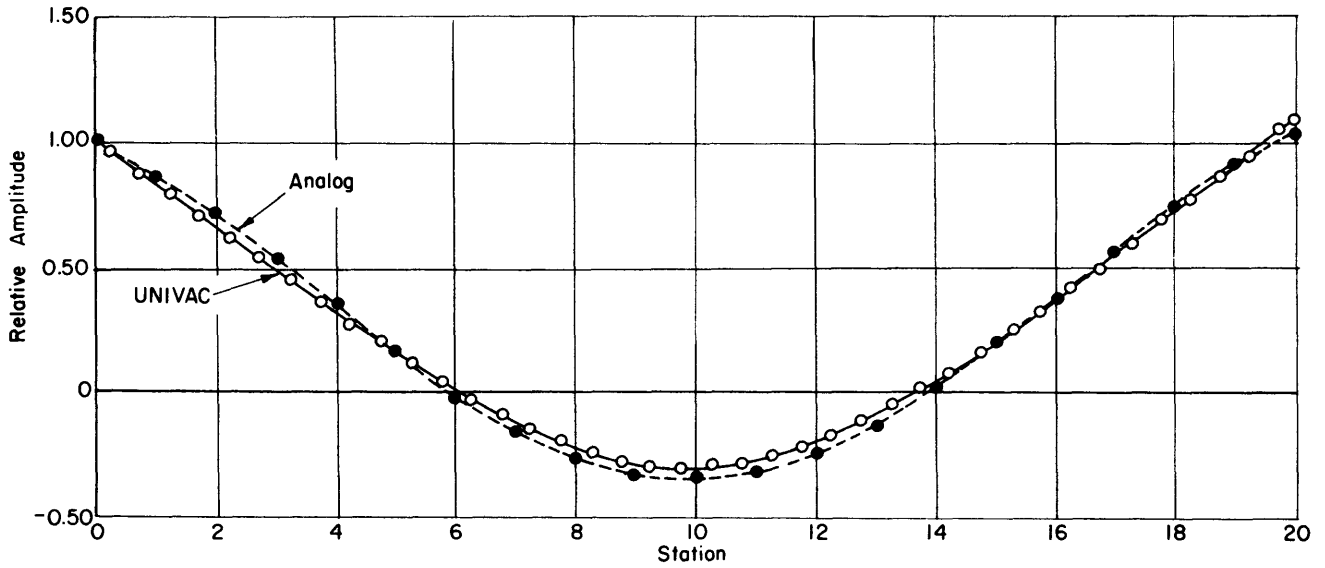


Figure 3a – 2-Noded Mode, 78.0 CPM

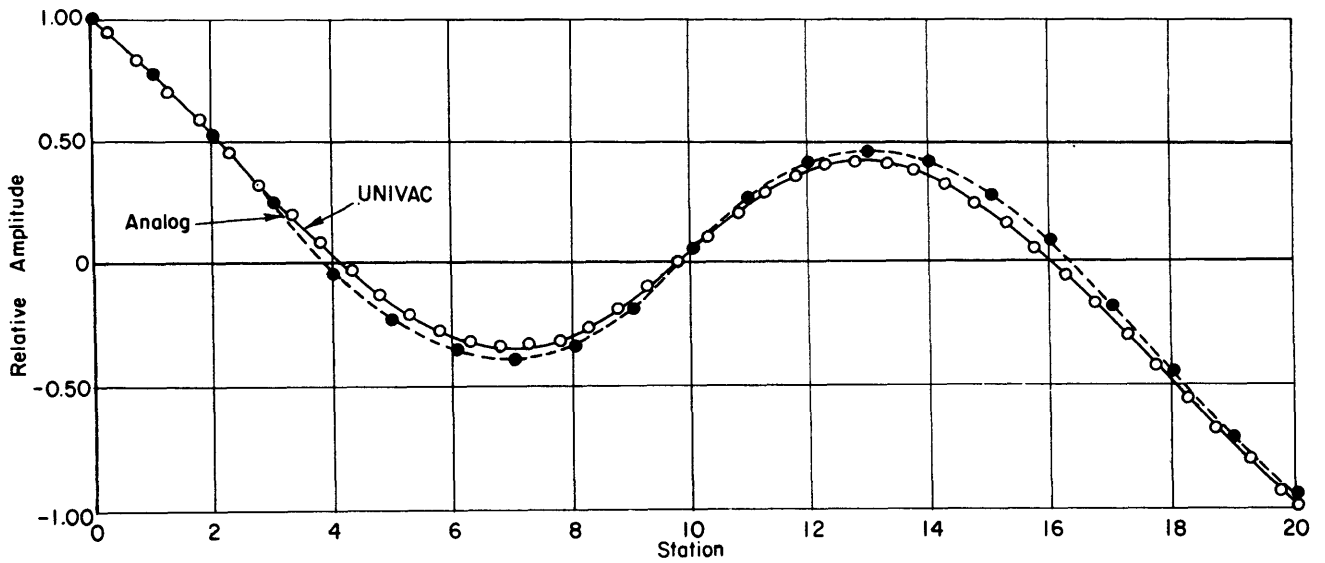


Figure 3b – 3-Noded Mode, 154.2 CPM

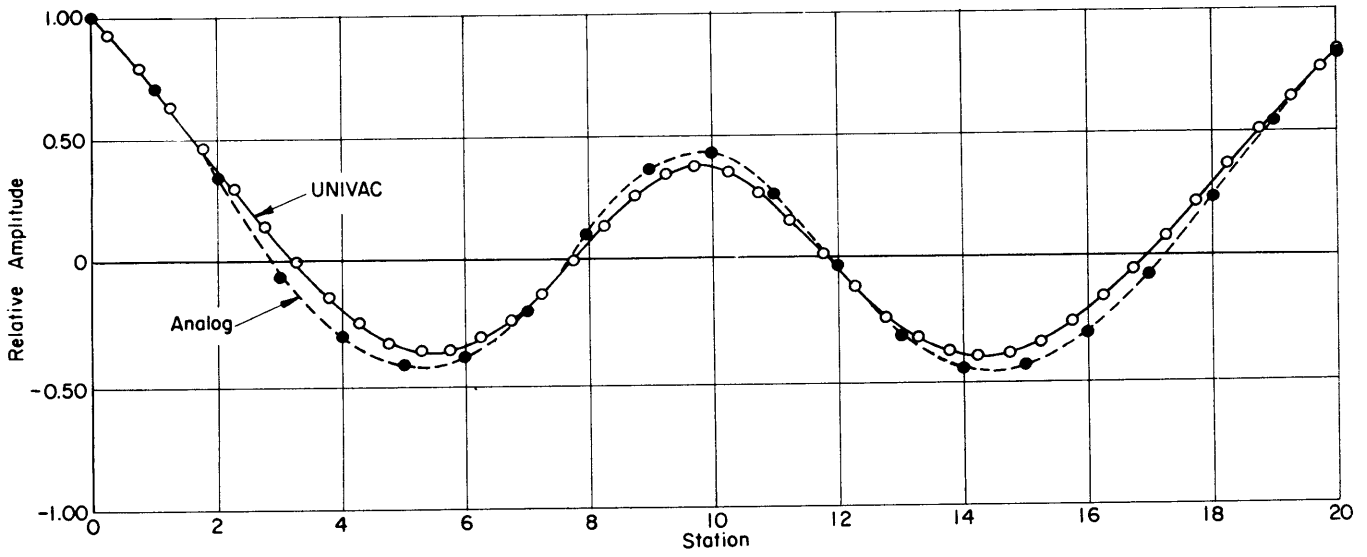


Figure 3c - 4-Noded Mode, 234.0 CPM

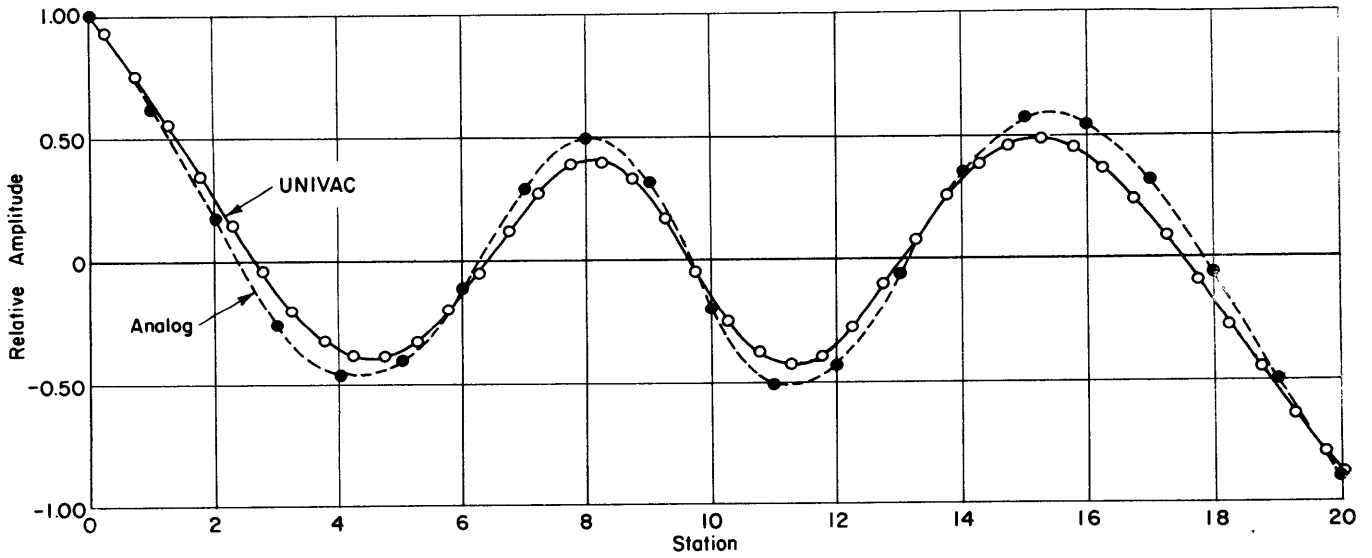


Figure 3d - 5-Noded Mode, 320.4 CPM

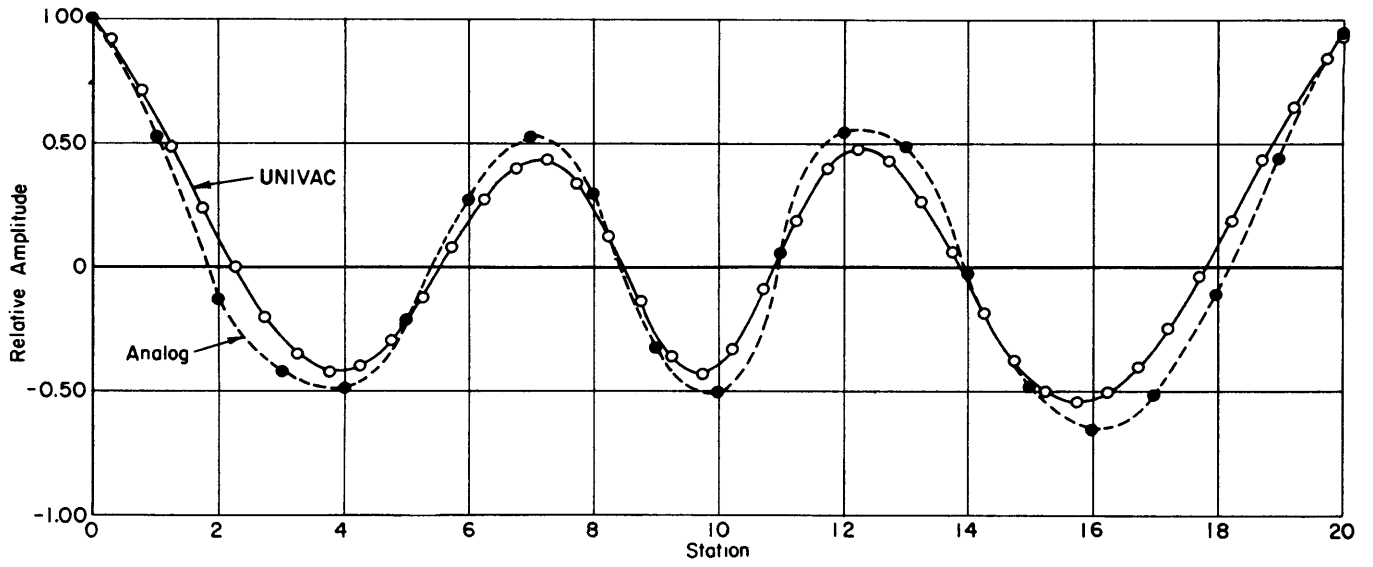


Figure 3e - 6-Noded Mode, 400.2 CPM

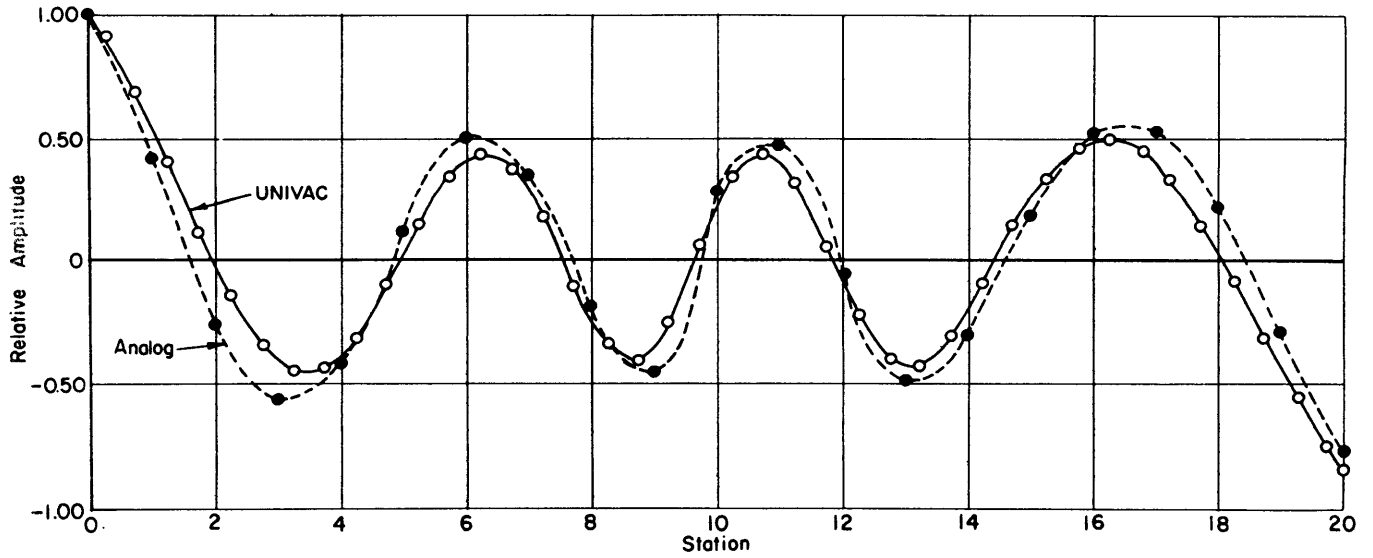


Figure 3f - 7-Noded Mode, 478.8 CPM

Figure 4 – Modes of Vertical Vibration of GOPHEF MARINER with and without a 10-Percent Sprung Mass Attached at Station 10 Determined by TMB Network Analyzer

The displacement was 18,674 tons corresponding to a condition of light load.

Wherever points and curves are not shown for the condition labeled “without sprung mass,” the curve and points labeled “with sprung mass” apply.

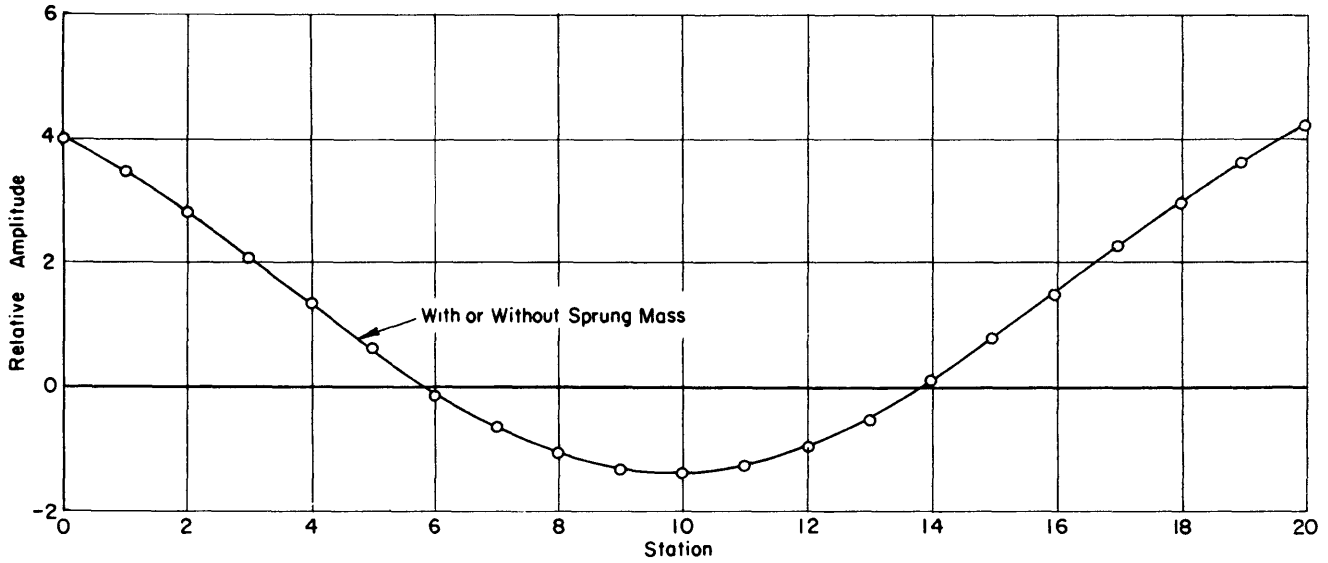


Figure 4a – 2-Noded Mode, 78.0 CPM

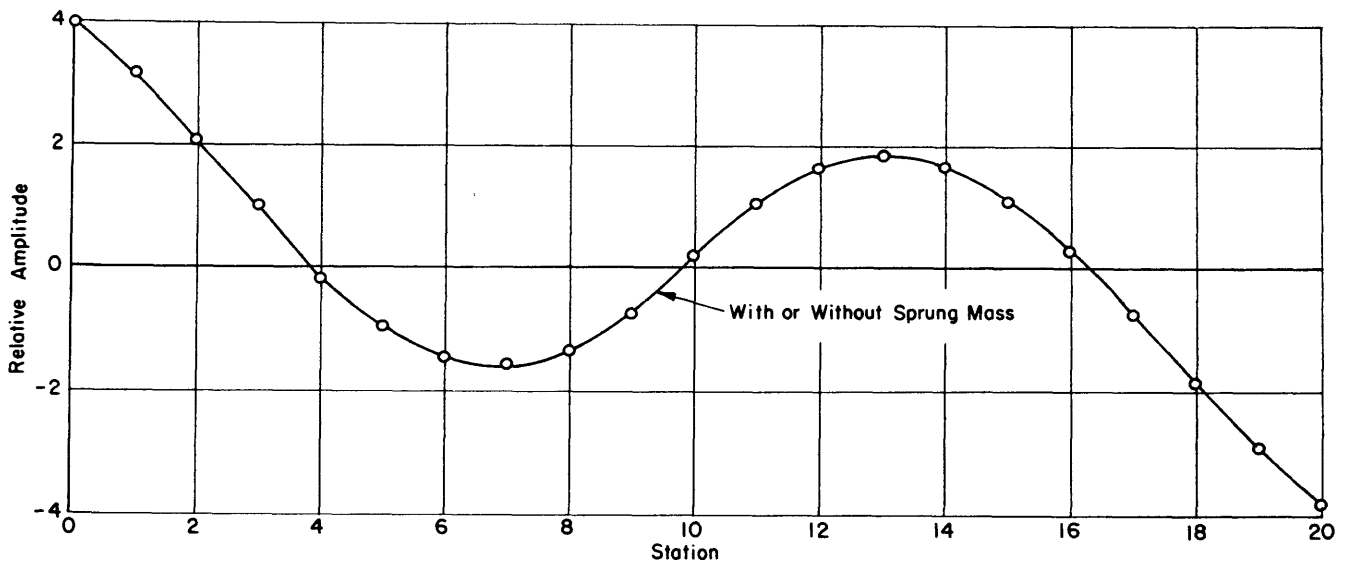


Figure 4b – 3-Noded Mode, 154.2 CPM

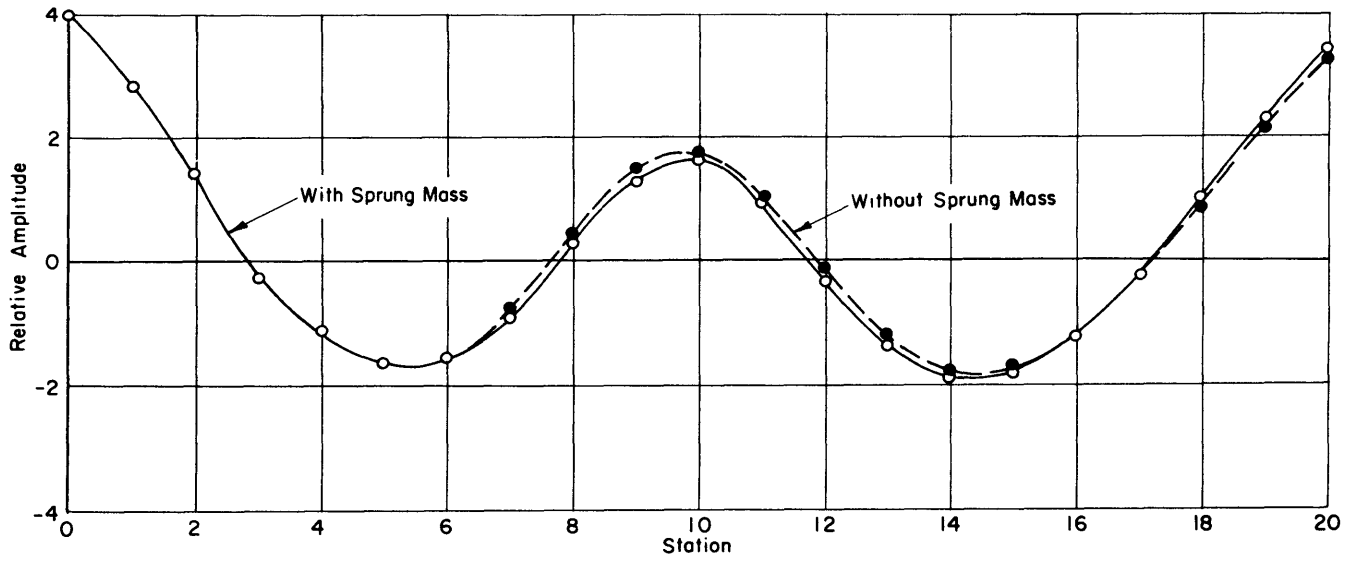


Figure 4c – 4-Noded Mode, 227.4 CPM

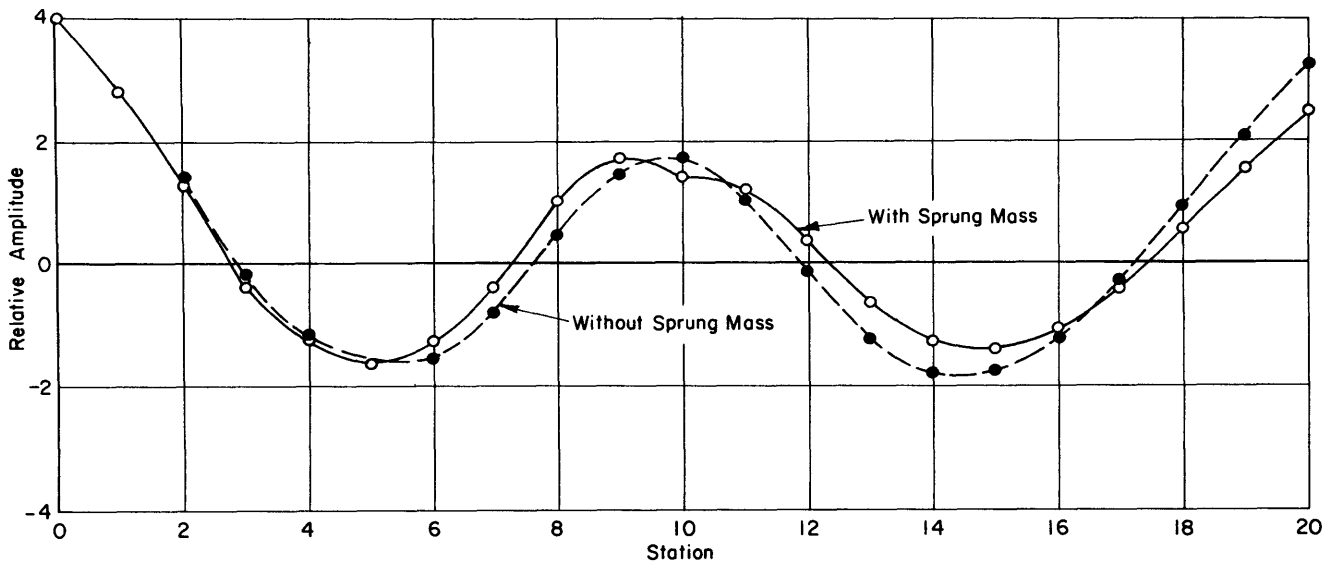


Figure 4d – 4-Noded Mode, 259.8 CPM

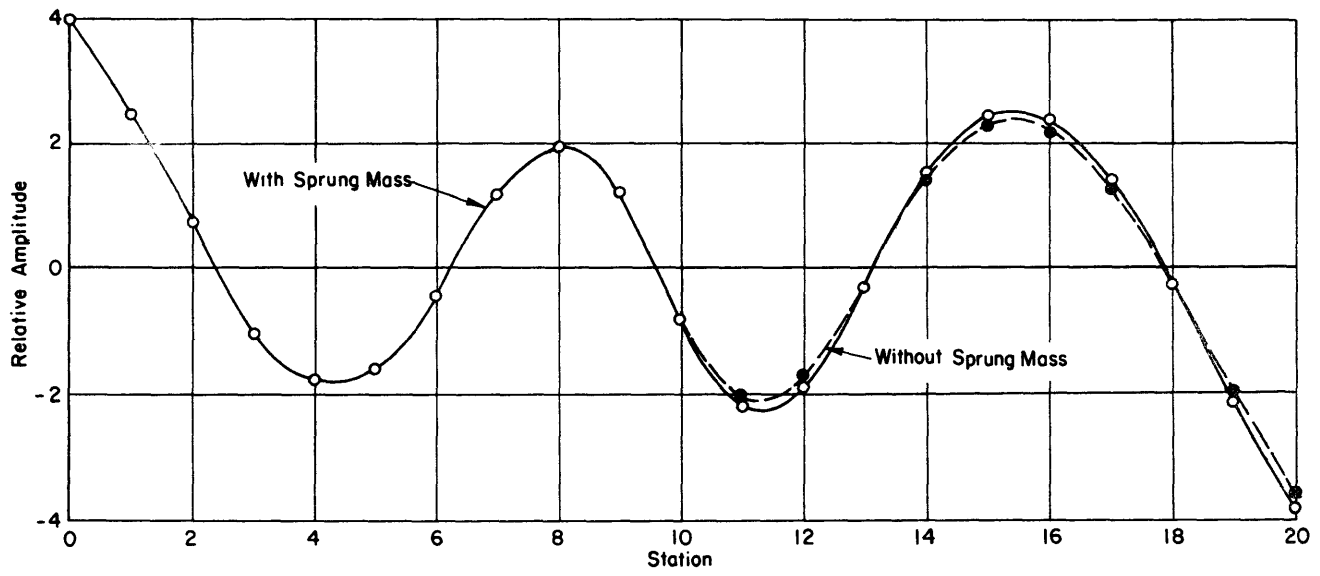


Figure 4e - 5-Noded Mode, 321.6 CPM

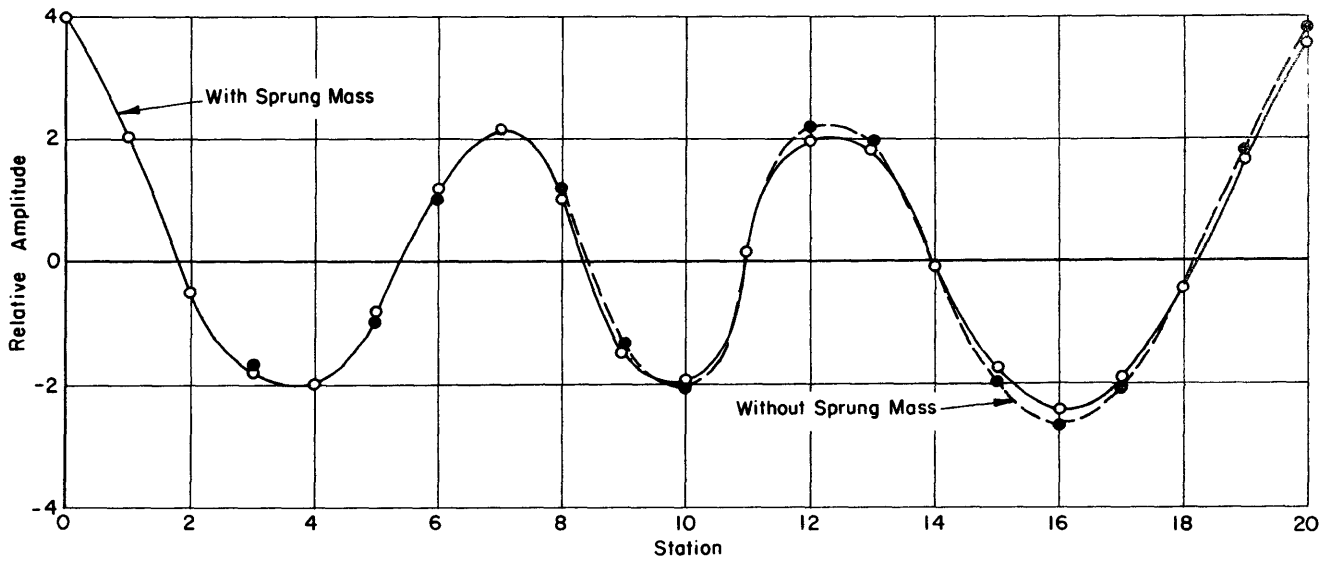


Figure 4f - 6-Noded Mode, 404.4 CPM

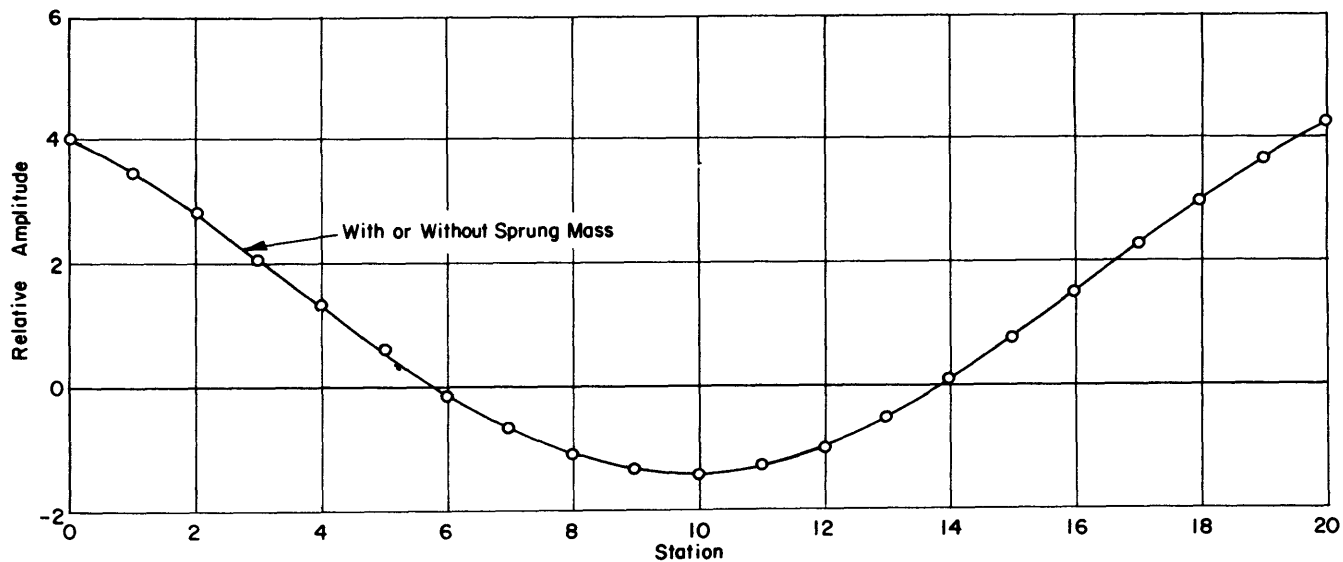


Figure 5a - 2-Noded Mode, 78.0 CPM

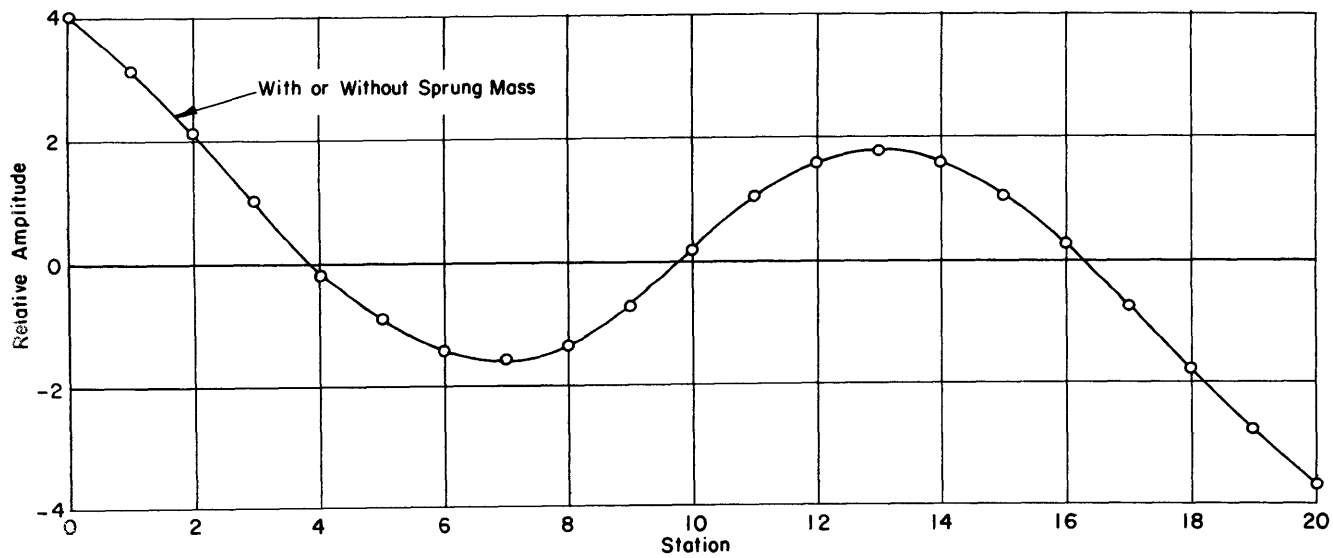


Figure 5b - 3-Noded Mode, 154.2 CPM



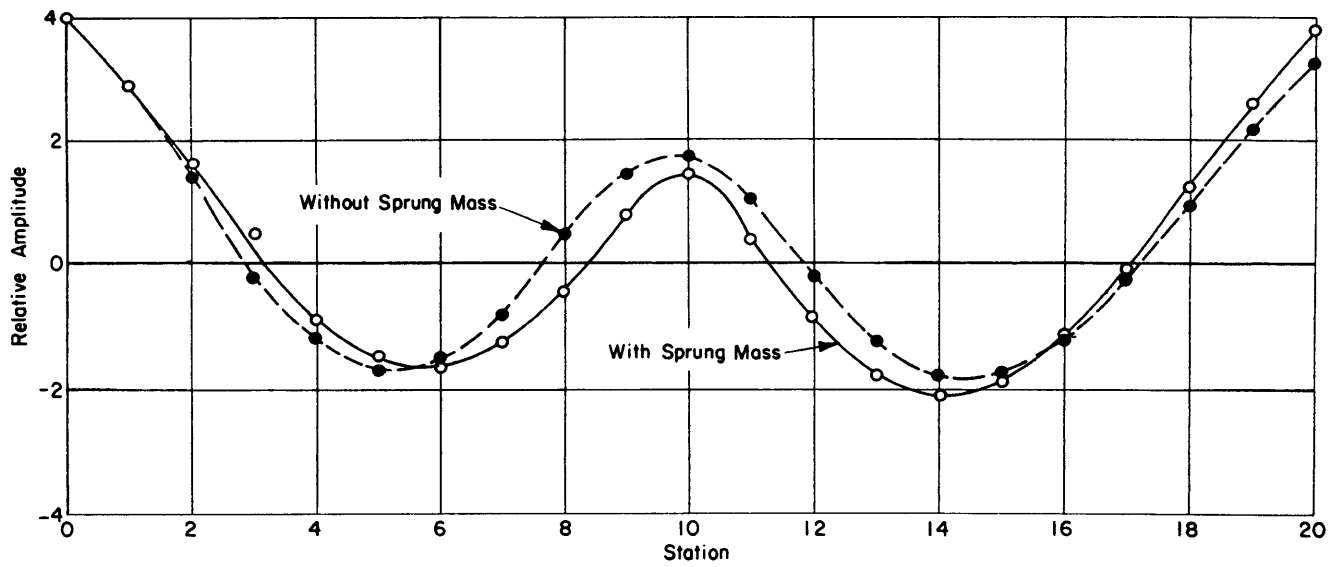


Figure 5c - 4-Noded Mode, 209.4 CPM

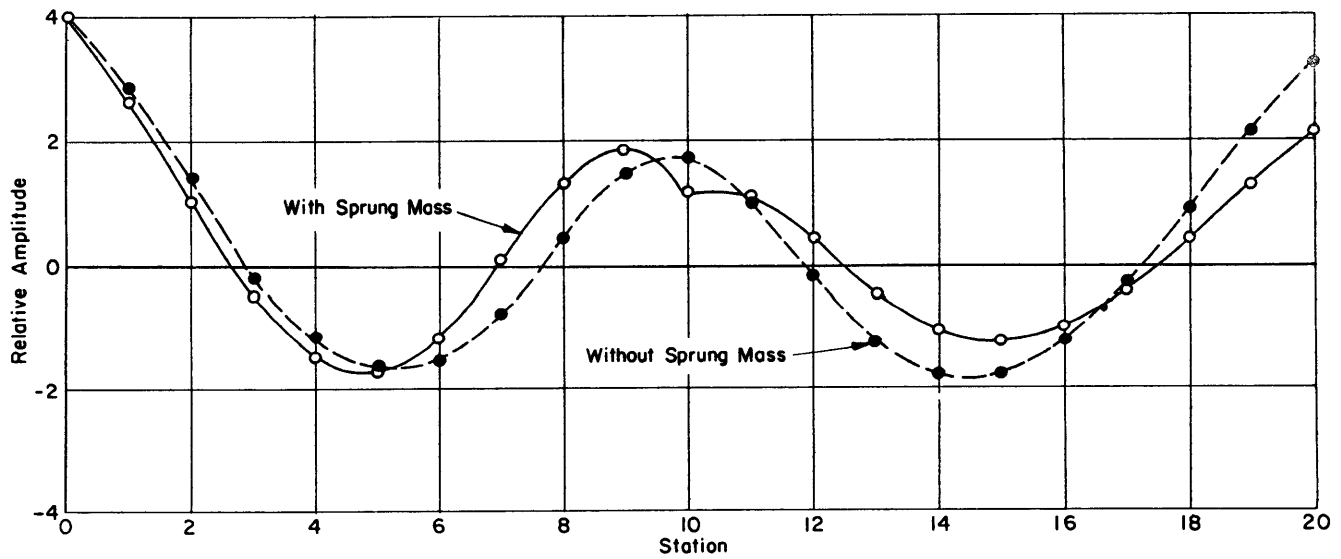


Figure 5d - 4-Noded Mode, 268.2 CPM

Figure 5 - Modes of Vertical Vibration of GOPHER MARINER with and without a 50-Percent Sprung Mass Attached at Station 10 Determined by TMB Network Analyzer

The displacement was 18,674 tons corresponding to a condition of light load.

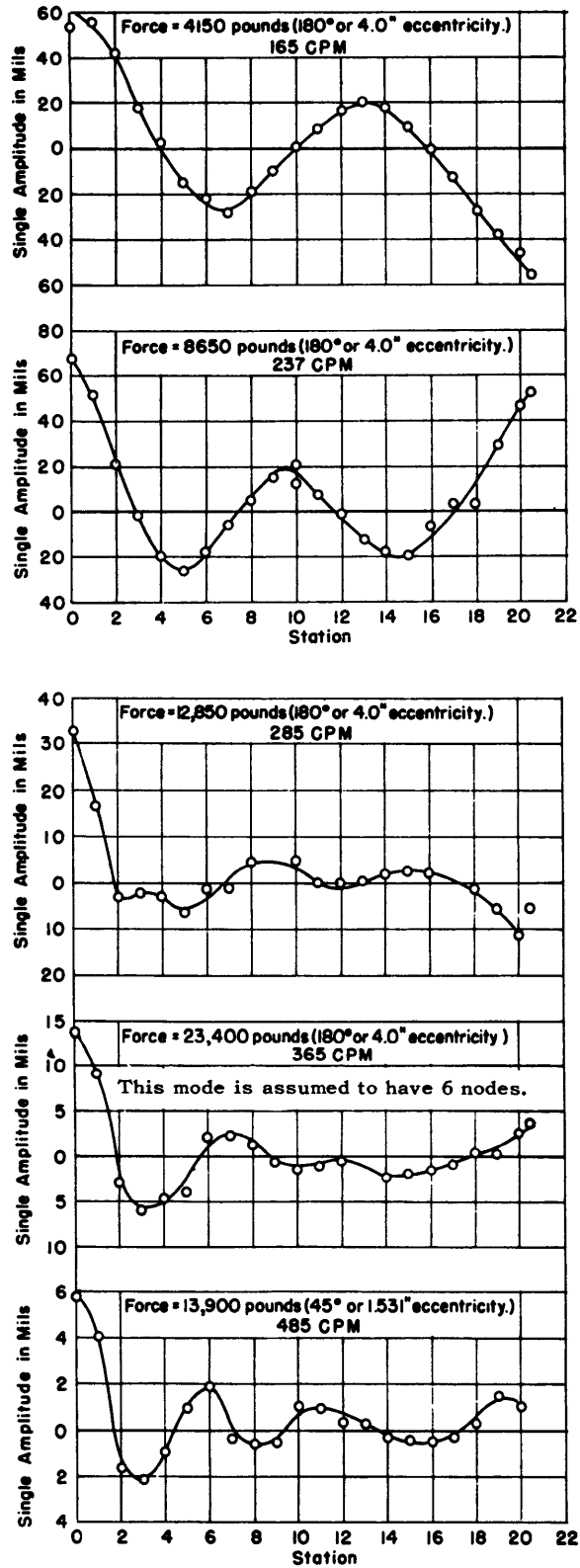


Figure 6 – Vertical-Amplitude Profiles of GOPHER MARINER Experimentally Obtained for Light-Loading Condition at Vibration Generator Speeds of 165, 237, 285, 365, and 485 RPM

This figure is adapted from Figure 19 of Reference 1.

#### 4. APPLICATION OF SPRUNG-MASS THEORY TO SS GOPHER MARINER

Inspection of Figure 6 shows that definite beamlike mode shapes could not be clearly established experimentally beyond the 4-noded mode of vertical vibration of GOPHER MARINER. From an analysis of these mode shapes it can be concluded that there are two with the same number of nodes. The mode *shapes* shown in Figures 4 and 5 for the beam with sprung mass also include two modes with the same number of nodes (6 nodes). Thus it is possible that the unusual mode *shapes* observed on GOPHER MARINER are the results of the effects of sprung masses.

#### 5. CONCLUSIONS

The following conclusions may be drawn from the analysis given in this report:

1. The TMB network analyzer may be used to explore accurately and quickly the effect of a single sprung mass upon the natural frequencies of a free-free uniform beam with bending flexibility only and negligible damping.
2. Analog results for the natural frequencies of uniform and shiplike nonuniform beam-sprung-mass systems with shear and bending flexibility are expected to be subject to errors of the same order of magnitude.
3. By inference the TMB network analyzer may be used also to determine the effects of many sprung masses upon the natural frequencies and mode shapes of a free-free nonuniform beam with shear and bending flexibility, rotary inertia, and damping. The system parameters may be readily changed on the analyzer, and a rapid exploration of their effects can be made.
4. The quantitative results obtained for the effects on the natural frequencies of a sprung mass on a beam are in accord with the qualitative theoretical predictions of Reference 4. Of particular interest are the facts that:
  - a. The original beam frequencies less than  $f_0$  are lowered by the addition of a sprung mass to the beam.
  - b. The original beam frequencies greater than  $f_0$  are raised by the addition of a sprung mass.
  - c. The amount of repulsion of the original beam frequencies increases with the magnitude of the sprung mass.
  - d. The original beam frequencies closest to  $f_0$  are repelled the most by the addition of the sprung mass.
  - e. A new natural frequency of the combined system is added which approaches  $f_0$  when the sprung mass is small, and deviates from  $f_0$  when the sprung mass is large.

5. Analog results for the mode shapes of a nonuniform beam are fairly accurate; see Figure 3.

6. In a beam-sprung-mass system the mode whose frequency is adjacent to and greater than  $f_0$  changes curvature rapidly; i.e., dips, at the point where the sprung mass is attached and the distance between the nodes adjacent to this point lengthens. For the mode whose frequency is adjacent to but less than  $f_0$  there is a peaking of the mode shape at the point of attachment and a contraction of the distance between the nodes adjacent to this point. The greater the sprung mass, the greater these effects.

## 6. ACKNOWLEDGMENTS

The author wishes to express his appreciation to Dr. N.H. Jasper and Dr. W.J. Sette for their critical and constructive review of this report. Dr. E.H. Kennard made valuable suggestions on the mathematical analysis presented herein. Mr. R.T. McGoldrick initially suggested that the TMB network analyzer be used to study the effect of a sprung mass on a beam. Mrs. B.H. Gesswein and Mr. A.W. McIver assisted in making analog measurements and numerical calculations.

## APPENDIX A

### RELATIONSHIP BETWEEN FORCE $F_p$ ACTING ON BEAM AND NATURAL FREQUENCIES OF COMBINED SPRUNG-MASS SYSTEM

The differential equation of motion of the mass  $m$  of Figure 1 during a *free vibration of the combined system* is<sup>3</sup>

$$m \frac{d^2 y_m}{dt^2} = -F_p = -m \omega_0^2 (y_m - y_p) \quad [5]$$

For steady free vibration of the combined system at circular frequency  $\omega$ ,

$$\frac{d^2 y_m}{dt^2} = -\omega^2 y_m \quad [6]$$

Substituting [6] in [5] gives

$$y_m = y_p \frac{\omega_0^2}{\omega_0^2 - \omega^2} \quad [7a]$$

or

$$y_m - y_p = y_p \left( \frac{\omega^2}{\omega_0^2 - \omega^2} \right) \quad [7b]$$

Then

$$F_p = m \omega_0^2 y_p \left( \frac{\omega^2}{\omega_0^2 - \omega^2} \right) \quad [8]$$

Equations [7] and [8] show that if  $\omega < \omega_0$ , the spring is in tension for positive  $y_p$ , and  $F_p$  is in phase with  $y_p$ . If  $\omega > \omega_0$ , the spring is in compression for positive  $y_p$ , and  $F_p$  is out of phase with  $y_p$ .

Equation [8] may be arranged in the form

$$F_p = \left[ m \left( \frac{\omega_0^2}{\omega_0^2 - \omega^2} \right) \right] \omega^2 y_p = m_e \omega^2 y_p \quad [9]$$

where  $m_e$  is the effective mass which, when added to the beam at point  $P$ , will have the same effect as the sprung mass  $m$  characterized by the circular frequency  $\omega_0$ . Note that  $m_e$  is positive for  $\omega < \omega_0$  and negative for  $\omega > \omega_0$ .

## APPENDIX B

### DERIVATION OF RESPONSE RATIO $y_p/F_p$ OF AN UNDAMPED FREE-FREE UNIFORM BEAM WITHOUT SHEAR AND WITH A SPRUNG MASS ATTACHED

Consider an undamped uniform beam without shear and with free ends (Figure 7). When such a beam vibrates at any point free from external force, its differential equation of motion is<sup>9</sup>

$$\mu \frac{\partial^2 y}{\partial t^2} + EI \frac{\partial^4 y}{\partial x^4} = 0 \quad [10]$$

where  $y$  is the *vertical* deflection,

$x$  is the distance from the origin of any point along the beam, and  
 $t$  is time.

Let a *vertical* sinusoidal force  $F = F_p \sin \omega t$  act on the beam at a point  $P$  which is at a distance  $x = b$  from the free left end of the beam located at  $x = 0$ . Steady forced vibrations only are considered. Then for  $x < b$  the solution of Equation [10] is

$$y = (B_1' \sin kx + B_1'' \cos kx + B_1''' \sinh kx + B_1^{iv} \cosh kx) \sin \omega t \quad [11]$$

where  $B_1'$ ,  $B_1''$ ,  $B_1'''$ , and  $B_1^{iv}$  are constants determined from the boundary conditions, and

$$k = \left( \frac{\mu \omega^2}{EI} \right)^{1/4}$$

Ignoring time variations and letting

$$y_x = \frac{\partial y}{\partial x}, \quad y_{xx} = \frac{\partial^2 y}{\partial x^2}, \quad y_{xxx} = \frac{\partial^3 y}{\partial x^3}$$

then

$$y = B_1' \sin kx + B_1'' \cos kx + B_1''' \sinh kx + B_1^{iv} \cosh kx \quad [12a]$$

$$y_x = k (B_1' \cos kx - B_1'' \sin kx + B_1''' \cosh kx + B_1^{iv} \sinh kx) \quad [12b]$$

$$y_{xx} = k^2 (-B_1' \sin kx - B_1'' \cos kx + B_1''' \sinh kx + B_1^{iv} \cosh kx) \quad [12c]$$

$$y_{xxx} = k^3 (-B_1' \cos kx + B_1'' \sin kx + B_1''' \cosh kx + B_1^{iv} \sinh kx) \quad [12d]$$

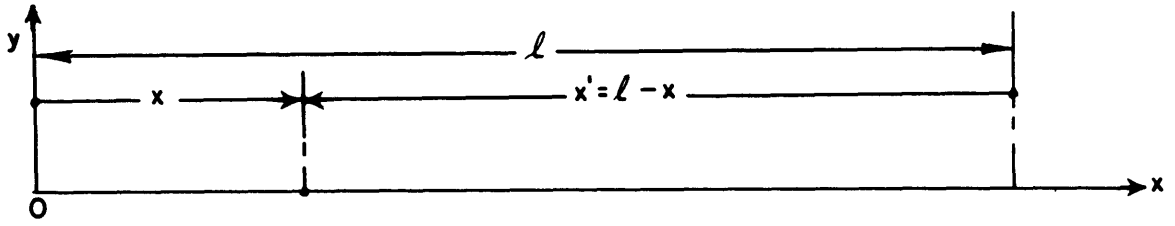


Figure 7 – Coordinate System with Origin at (0,0)

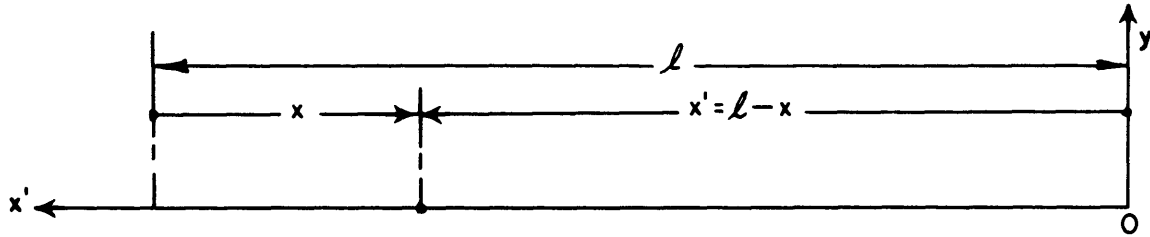


Figure 8 – Coordinate System with Origin at (l, 0)

The boundary conditions at  $x = 0$  are  $y_{xx} = 0, y_{xxx} = 0$ .

Hence  $B_1'' = B_1^{iv}; B_1' = B_1'''$

For later use it is easily concluded that at  $x = b$

$$\frac{1}{2} \left( y + \frac{y_{xx}}{k^2} \right) = B_1' \sinh kb + B_1'' \cosh kb \quad [13a]$$

$$\frac{1}{2} \left( y - \frac{y_{xx}}{k^2} \right) = B_1' \sin kb + B_1'' \cos kb \quad [13b]$$

$$\frac{1}{2} \left( \frac{y_x}{k} + \frac{y_{xxx}}{k^3} \right) = B_1' \cosh kb + B_1'' \sinh kb \quad [13c]$$

$$\frac{1}{2} \left( \frac{y_x}{k} - \frac{y_{xxx}}{k^3} \right) = B_1' \cos kb - B_1'' \sin kb \quad [13d]$$



Now consider the section of the beam to the right of  $x = b$  and let  $x' = l - x$ . Thus  $x'$  is the distance from the right end of the beam to the point  $x$  as shown in Figure 7.

Now consider that the origin of  $x'$  exists at the right end of the beam, which is also free, and that a positive  $x'$  axis extends to the left as shown in Figure 8.

Expressions similar to Equations [12] may be written for  $y, y_x, y_{xx}, y_{xxx}$  in this new coordinate system with  $B_2' = B_2'''$  and  $B_2'' = B_2^{iv}$  evaluated for the boundary conditions at  $x' = 0$ .

Thus

$$y = B_2' \sin k(l - x) + B_2'' \cos k(l - x) + B_2' \sinh k(l - x) + B_2'' \cosh k(l - x) \quad [14a]$$

$$y_x = k [-B_2' \cos k(l - x) + B_2'' \sin k(l - x) - B_2' \cosh k(l - x) - B_2'' \sinh k(l - x)] \quad [14b]$$

$$y_{xx} = k^2 [-B_2' \sin k(l - x) - B_2'' \cos k(l - x) + B_2' \sinh k(l - x) + B_2'' \cosh k(l - x)] \quad [14c]$$

$$y_{xxx} = k^3 [B_2' \cos k(l - x) - B_2'' \sin k(l - x) - B_2' \cosh k(l - x) - B_2'' \sinh k(l - x)] \quad [14d]$$

At  $x = b$  or  $x' = l - b$

$$\frac{1}{2} \left( y + \frac{y_{xx}}{k^2} \right) = B_2' \sinh k(l - b) + B_2'' \cosh k(l - b) \quad [15a]$$

$$\frac{1}{2} \left( y - \frac{y_{xx}}{k^2} \right) = B_2' \sin k(l - b) + B_2'' \cos k(l - b) \quad [15b]$$

$$\frac{1}{2} \left( \frac{y_x}{k} + \frac{y_{xxx}}{k^3} \right) = -B_2' \cosh k(l - b) - B_2'' \sinh k(l - b) \quad [15c]$$

$$\frac{1}{2} \left( \frac{y_x}{k} - \frac{y_{xxx}}{k^3} \right) = -B_2' \cos k(l - b) + B_2'' \sin k(l - b) \quad [15d]$$

The beam may now be regarded as two equivalent beams joined by an element of differential length  $dx$  (see Figure 9) which finally is made to approach zero. We will then have the actual beam. Figure 9 shows the momentary direction of the shearing forces  $V_1$  and  $V_2$  and the moments  $M_1$  and  $M_2$  acting on the beam corresponding to a force  $F_p$  acting on the differential element  $dx$ . The dotted line indicates the deflection curve at the particular instant when the

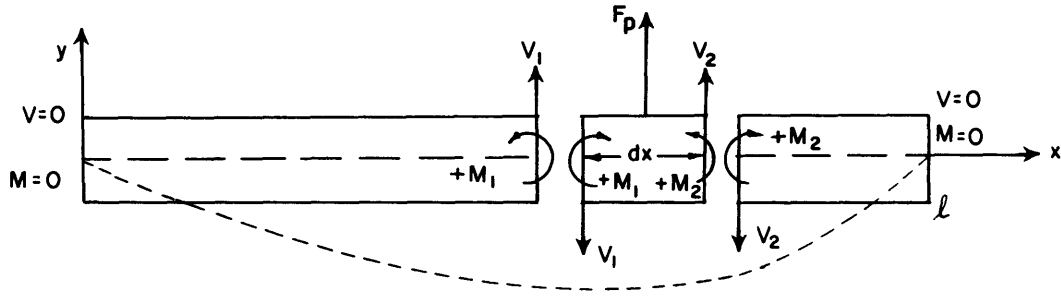


Figure 9 – Sign Convention for Moments and Forces Acting on Beam

shearing forces and moments are as shown. With the deflection curve as shown, there are bending moments producing compression in the upper fibers of the beam.

Figure 9 also shows the sign convention that has been adopted. Compression in the upper fibers is regarded as positive. Also, an upward shearing force  $V_1$  acting on the beam to the left of a cross section and a downward shearing force  $V_1$  acting on the beam to the right of that cross section are regarded as positive and similarly for  $V_2$ . It is clear that according to this sign convention the actual bending moments and shearing forces in Figure 9 are positive. The quantity  $y_{xx}$  is also positive. When  $dx \rightarrow 0$

$$M_1 = EI (y_{xx})_L \rightarrow M_2 = EI (y_{xx})_R \quad [16]$$

or

$$(y_{xx})_L \rightarrow (y_{xx})_R \quad [17]$$

It is clear that  $y_{xx}$  is continuous.

Equilibrium of the forces on the  $dx$  element requires that

$$F_p = V_1 - V_2 = -EI (y_{xxx})_L + EI (y_{xxx})_R \quad [18]$$

or

$$\left( \frac{-y_{xxx}}{k^3} \right)_L + \left( \frac{y_{xxx}}{k^3} \right)_R = \frac{F_p}{k^3 EI} \quad [19]$$

Let

$$\begin{aligned}
 s_1 &= \sin kb; & s_2 &= \sin k(l-b) \\
 c_1 &= \cos kb; & c_2 &= \cos k(l-b) \\
 S_1 &= \sinh kb; & S_2 &= \sinh k(l-b) \\
 C_1 &= \cosh kb; & C_2 &= \cosh k(l-b)
 \end{aligned}$$

Now  $\left(\frac{y_{xxx}}{k^3}\right)_L$  and  $\left(\frac{y_{xxx}}{k^3}\right)_R$  may be found from the difference in Equations [13c] and

[13d] and [15c] and [15d], respectively.

Substitution of these differences into Equation [19] gives

$$-B_1'(C_1 - c_1) - B_1''(S_1 + s_1) - B_2'(C_2 - c_2) - B_2''(S_2 + s_2) = \frac{F_p}{k^3 EI} \quad [20]$$

Since  $y, y_x, y_{xx}$  are continuous at  $x = b$ , then equations for  $\frac{1}{2}\left(y + \frac{y_{xx}}{k^2}\right)$  and  $\frac{1}{2}\left(y - \frac{y_{xx}}{k^2}\right)$

are also continuous. The continuity of  $y_x$  permits the sum of Equations [13c] and [13d] to be equated to the sum of Equations [15c] and [15d]. The continuity of

$\frac{1}{2}\left(y \pm \frac{y_{xx}}{k^2}\right)$  permits Equations [13a] and [15a] and Equations [13b] and [15b] to be equated.

Thus

$$B_1'(C_1 + c_1) + B_1''(S_1 - s_1) = -B_2'(C_2 + c_2) - B_2''(S_2 - s_2) \quad [21]$$

$$S_1 B_1' + C_1 B_1'' - S_2 B_2' - C_2 B_2'' = 0 \quad [22]$$

$$s_1 B_1' + c_1 B_1'' - s_2 B_2' - c_2 B_2'' = 0 \quad [23]$$

Equations [20] and [21] may be added and subtracted to give the following simpler equations:

$$c_1 B_1' - s_1 B_1'' + c_2 B_2'' - s_2 B_2' = \frac{F_p}{2k^3 EI} \quad [24]$$

$$C_1 B_1' + S_1 B_1'' + C_2 B_2' + S_2 B_2'' = \frac{-F_p}{2k^3 EI} \quad [25]$$

Equations [22], [23], [24], and [25] are four linear algebraic equations which may be solved for the four unknown constants  $B_1'$ ,  $B_1''$ ,  $B_2'$ , and  $B_2''$  by means of determinants. However, these equations need be solved only for  $B_1'$  and  $B_1''$  to find the response ratio  $y_p/F_p$  since  $B_1'' = B_1^{iv}$  and  $B_1' = B_1''''$ . Then upon substitution of  $x = b$  in Equation [12a] we have

$$y_p = B_1'(S_1 + s_1) + B_1''(C_1 + c_1) \quad [26]$$

For convenience, Equations [22], [23], [24], and [25] are regrouped

$$S_1 B_1' + C_1 B_1'' - S_2 B_2' - C_2 B_2'' = 0 \quad [22]$$

$$s_1 B_1' + c_1 B_1'' - s_2 B_2' - c_2 B_2'' = 0 \quad [23]$$

$$c_1 B_1' - s_1 B_1'' + c_2 B_2' - s_2 B_2'' = \frac{F_p}{2k^3 EI} \quad [24]$$

$$C_1 B_1' + S_1 B_1'' + C_2 B_2' + S_2 B_2'' = \frac{-F_p}{2k^3 EI} \quad [25]$$

We solve for  $B_1'$  and  $B_1''$  by the method of determinants and obtain

$$B_1' = \frac{-F_p}{2k^3 EI} \frac{\begin{bmatrix} -S_2 (s_1 c_2 + c_1 s_2) - C_2 (c_1 c_2 - s_1 s_2) + C_1 (s_2^2 + c_2^2) \\ + c_2 (S_1 S_2 + C_1 C_2) - c_1 (C_2^2 - S_2^2) - s_2 (C_1 S_2 + S_1 C_2) \end{bmatrix}}{2 (1 - \cos kl \cosh kl)} \quad [27]$$

and

$$B_1'' = \frac{F_p}{2k^3 EI} \frac{\begin{bmatrix} S_2 (c_1 c_2 - s_1 s_2) - C_2 (c_2 s_1 + c_1 s_2) + S_1 (s_2^2 + c_2^2) \\ + c_2 (C_1 S_2 + S_1 C_2) - s_1 (C_2^2 - S_2^2) - s_2 (S_1 S_2 + C_1 C_2) \end{bmatrix}}{2 (1 - \cos kl \cosh kl)} \quad [28]$$

Substitute  $B_1'$  and  $B_1''$  in Equation [26] and equate to unity  $s_2^2 + c_2^2$  and  $C_2^2 - S_2^2$  in Equations [27] and [28]. Most terms cancel and the remainder, upon division by  $F_p$ , is the desired response ratio:

$$\frac{y_p}{F_p} = \frac{1}{2k^3 EI} \frac{\begin{bmatrix} \cos k(l-b) \sinh k(l-b) - \sin k(l-b) \cosh k(l-b) \\ + \cos k(l-b) \cos kb \sinh kl - \sin kl \cosh kb \cosh k(l-b) \\ + \cos kb \sinh kb - \sin kb \cosh kb \end{bmatrix}}{(1 - \cos kl \cosh kl)} \quad [29]$$

## APPENDIX C

### ELECTRICAL ANALOG OF A UNIFORM BEAM-SPRUNG-MASS SYSTEM

The natural frequencies of an undamped free-free uniform beam without sprung mass and with bending flexibility only may easily be computed by the network analyzer.<sup>5</sup> Figure 10 shows the 20-section analog of the uniform GOPHER MARINER beam. The conversion or scaling factors<sup>5</sup> used in transforming mechanical parameters to electrical parameters are  $\alpha = 3.4 \times 10^7$ ,  $\beta = 5 \times 10^4$ ,  $\lambda = 2 \times 10^{-9}$ ,  $\tau = 26.25$ ,  $\nu = 100$  where

$$\alpha = \frac{\left(\frac{\Delta x}{EI}\right)'}{\left(\frac{\Delta x}{EI}\right)}$$

$$\beta = \frac{\left(\frac{\Delta x}{KAG}\right)'}{\left(\frac{\Delta x}{KAG}\right)}$$

$$\lambda = \frac{m_n'}{m_n}$$

$$\tau = \frac{\Delta x}{(\Delta x)'}$$

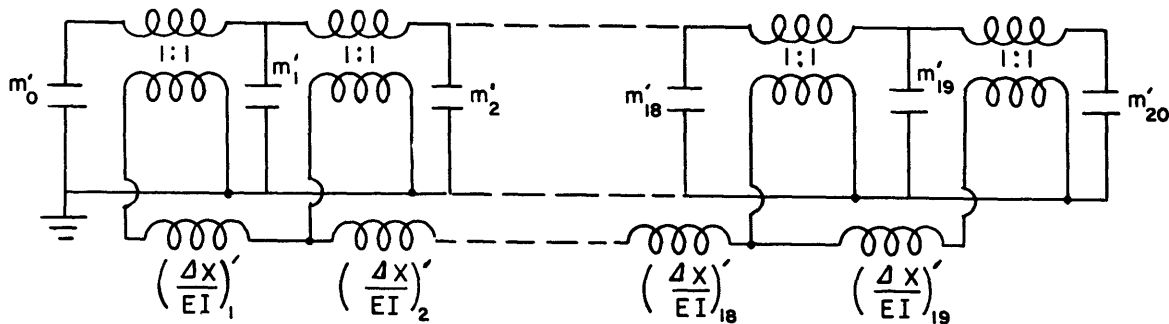


Figure 10 – Analog of Uniform GOPHER MARINER Beam with Bending Flexibility only and without Sprung Mass  
The analog used comprised 20 sections.

The electrical parameters are  $m'_0 = 0.092 \mu f$ ,  $m'_1 = m'_2 = \dots = m'_{19} = 0.183 \mu f$ ,  $m'_{20} = 0.092 \mu f$  and

$$\left(\frac{\Delta x}{EI}\right)'_1 = \left(\frac{\Delta x}{EI}\right)'_2 = \dots = \left(\frac{\Delta x}{EI}\right)'_{19} = 0.06 h. \quad \text{All transformer turn ratios} = 1:1.$$

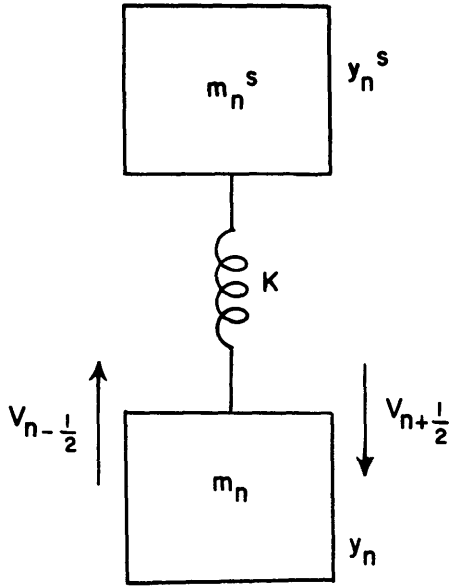


Figure 11 – Sprung-Mass System

momentary direction of the shearing forces. Consider  $y_n$  and  $y_n^s$  as positive in the direction of the increasing ordinate (upwards) with respect to the static equilibrium condition.

$$m_n \ddot{y}_n = V_{n-1/2} - V_{n+1/2} + K(y_n^s - y_n) \quad [30]$$

$$j\omega m_n \dot{y}_n = V_{n-1/2} - V_{n+1/2} + \frac{K}{j\omega} (\dot{y}_n^s - \dot{y}_n) \quad [31]$$

$$V_{n+1/2} - V_{n-1/2} = -j\omega m_n \dot{y}_n + \frac{K}{j\omega} (\dot{y}_n^s - \dot{y}_n) \quad [32]$$

$$m_n^s \ddot{y}_n^s = K(y_n - y_n^s) \quad [33]$$

$$j\omega m_n^s \dot{y}_n^s = \frac{K}{j\omega} (\dot{y}_n - \dot{y}_n^s) \quad [34]$$

These equations may be represented by an electrical mobility analog which has been added to Station 10 ( $n = 10$ ) of Figure 10, as shown in Figure 12,

where  $m_n^s$  is represented by capacitance  $(m_n^s)'$

$K$  is represented by inductance  $\left(\frac{1}{K}\right)'$

$y_n^s$  is represented by time integral of voltage  $(y_n^s)'$

For this beam the natural frequencies measured on the TMB network analyzer are given in Table 1.

We now consider the addition of a sprung mass to the analog of the uniform GOPHER MARINER beam. For this beam the critical frequencies measured on the TMB network analyzer are also given in Table 1.

The derivation of an electrical analog system equivalent to the sprung-mass system of Figure 11 may be obtained by using Newton's laws for the analysis of the sprung-mass system. The solution to the dynamics problem can then be represented by an electrical mobility analog.

This analysis is now made for a free vibration.

In Figure 11 let  $V_{n-1/2}$  and  $V_{n+1/2}$  represent the

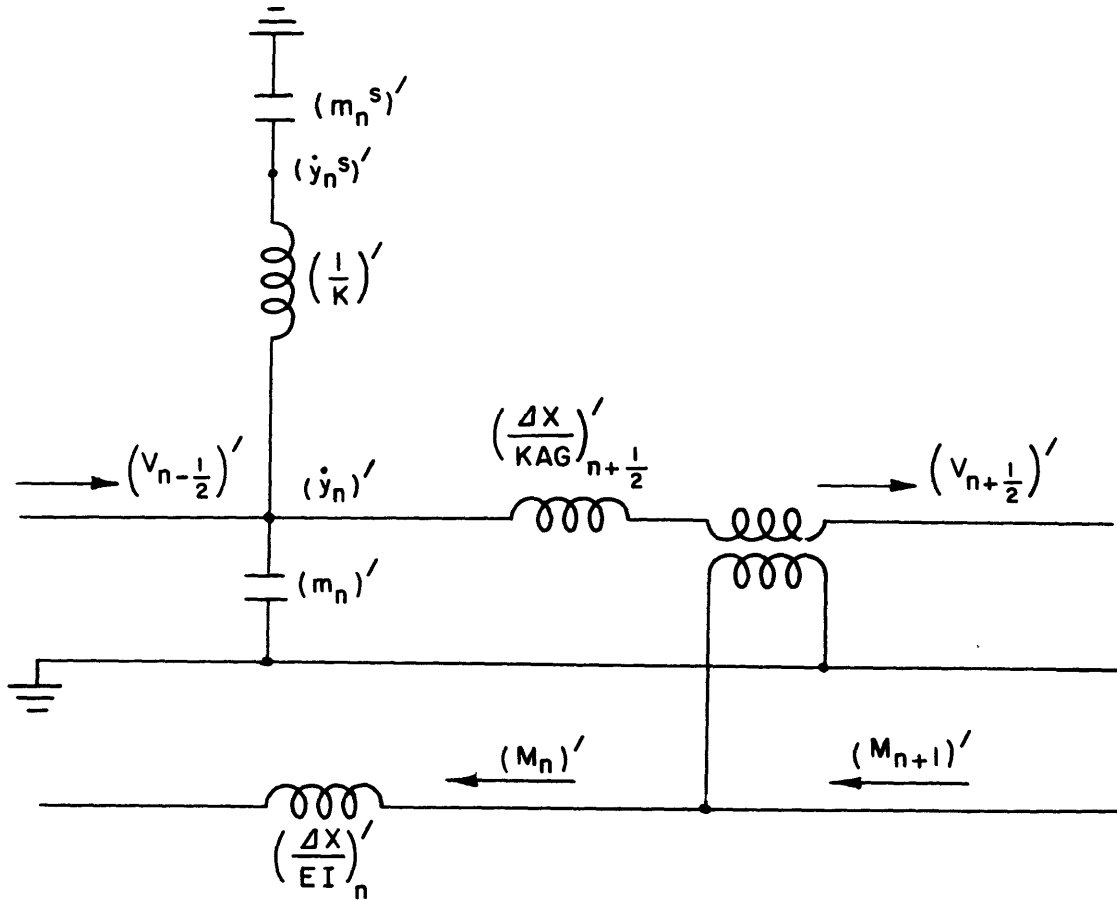


Figure 12 – Sprung-Mass Mobility Analog Added at Station  $n = 10$ , to 20-Section Analog Shown in Figure 10

$\dot{y}_n^s$  is represented by voltage  $(\dot{y}_n^s)'$

$\ddot{y}_n^s$  is represented by derivative of voltage  $(\ddot{y}_n^s)'$

$$(\omega_0^s)^2 = \frac{K}{m_n^s} \text{ or } (\omega_0^s)^2 m_n^s = K \quad [35]$$

The relationship between electrical and mechanical parameters is given by Reference 5.

$$(m_n^s)' = \lambda m_n^s \text{ or } m_n^s = \frac{(m_n^s)'}{\lambda} \quad [36]$$

and

$$(\omega_0^s)' = \nu \omega_0^s \text{ or } \omega_0^s = \frac{(\omega_0^s)'}{\nu} \quad [37]$$

Then, substituting [36] and [37] in [35], we find that

$$\frac{[(\omega_0^s)']^2 (m_n^s)'}{\lambda \nu^2} = K \quad [38]$$

$$[(\omega_0^s)']^2 (m_n^s)' = \lambda \nu^2 K = K' \quad [39]$$

Dimensional homogeneity requires that  $\lambda \nu^2 K = K'$  be an electrical quantity. The reciprocal of  $K'$  has been denoted in Figure 12 by  $\left(\frac{1}{K}\right)'$ , the electrical value of the spring constant.

The capacitance and inductance  $(m_n^s)'$  and  $K'$  or  $\left(\frac{1}{K}\right)'$  are obtained from Equations [36] and [39], respectively.



## APPENDIX D

### ACCURACY OF FREQUENCY CORRESPONDING TO ADDED MODE FOR UNDAMPED FREE-FREE UNIFORM BEAM WITH SPRUNG MASS ATTACHED

For the undamped free-free uniform beam with bending flexibility only, the measured and theoretical values of the additional frequency  $f_{3a}$  agree closely, within 0.88 percent, as shown in Table 1. The unusually good accuracy can be qualitatively understood from a consideration of Figure 13, which shows the response ratio  $y_p/F_p$  plotted against  $f$  for both the free-free beam and the sprung mass alone.

In Figure 13, Curve A is theoretically exact, and Curve B is obtained on the network analyzer. An error in a resonance frequency determined on the analyzer appears as a horizontal displacement of the response curves at the points of maximum response; i.e., at  $f_4^a$  and  $f_4^t$ .

The response curve for the sprung mass represents both theoretical and experimental values, since the analog for the sprung mass is precise. It crosses the horizontal axis at  $f_0$ . The resonance frequencies for the combined system correspond to the frequencies at which the curve for the sprung mass intersects the response curves for the beam. It is evident that  $f^a$  differs from  $f^t$  but that, because of the vertical tilt of the curve for the spring-mass system, the difference between the theoretical and experimental value is reduced. For a small sprung mass the curve is very steep, and the difference would be very small.

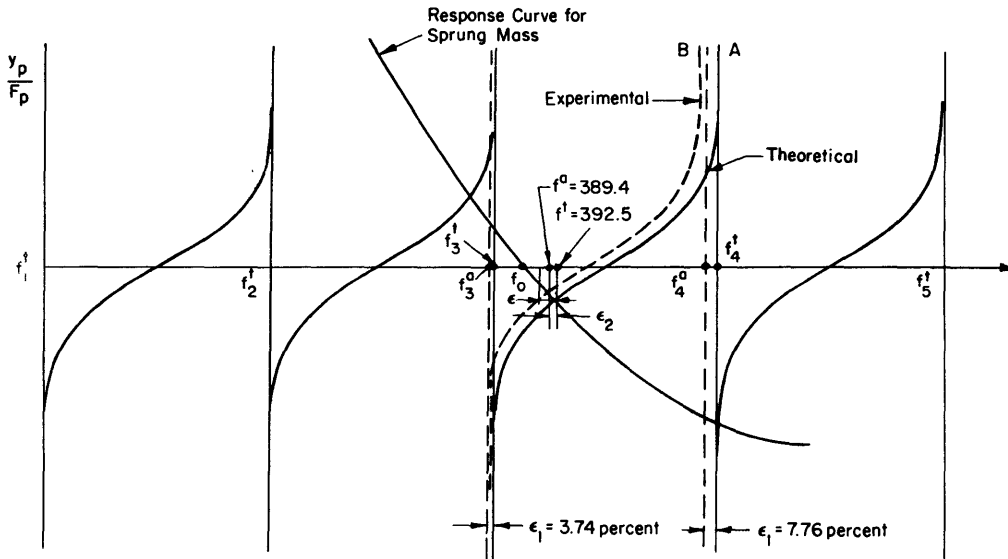


Figure 13 – Response Ratios for a Beam and a Sprung Mass as a Function of Frequency

- $f^t$  is the theoretically exact value of  $f_{3a}$ ,
- $f^a$  is the TMB network analyzer value of  $f_{3a}$ ,
- $f_0$  is the natural frequency of free vibration of the mass-spring system alone,
- $f_3^t, f_4^t$  are theoretically exact values of frequencies adjacent to  $f_0$ , and
- $f_3^a, f_4^a$  are TMB network analyzer values of frequencies adjacent to  $f_0$ .



## APPENDIX E

### ELECTRICAL ANALOG OF NONUNIFORM BEAM-SPRUNG-MASS SYSTEM

The data used in obtaining a 20-section analog of the nonuniform GOPHER MARINER beam are shown in Table 3. The corresponding analog of the beam with an attached sprung mass is shown in Figure 14. The principal characteristics of the GOPHER MARINER are:

Length between perpendiculars	525 ft
Beam	76 ft
Depth	44 ft 6 in.
Design draft	27 ft
Design displacement	18,674 tons

TABLE 3

Data for Analog of 20-Section Nonuniform GOPHER MARINER Beam  
with Bending and Shearing Flexibility

These data are for light loading vertical vibration condition.

Station	$\frac{m_n}{\text{ton-sec}^2}$ ft	$\frac{\Delta x}{EI} \times 10^8$ (ton-ft) <sup>-1</sup>	$\frac{\Delta x}{KAG} \times 10^6$ ft/ton	$m'_n$ $\mu f$	$\left(\frac{\Delta x}{EI}\right)'_n$ h	$\left(\frac{\Delta x}{KAG}\right)'_n$ h
0	7.39	0.3160		0.015	0.177	0.568
1	12.26	0.5205	11.35	0.025	0.123	0.428
2	17.90	0.3615	8.56	0.036	0.098	0.359
3	31.43	0.2880	7.17	0.063	0.083	0.338
4	45.33	0.2455	6.75	0.091	0.074	0.286
5	61.31	0.2185	5.72	0.123	0.068	0.284
6	60.39	0.2005	5.67	0.121	0.064	0.304
7	68.38	0.1880	6.08	0.137	0.061	0.335
8	83.45	0.1800	6.70	0.167	0.060	0.362
9	89.96	0.1760	7.23	0.180	0.060	0.381
10	91.61	0.1750	7.62	0.183	0.060	0.387
11	69.03	0.1750	7.73	0.138	0.061	0.382
12	64.44	0.1790	7.63	0.129	0.064	0.369
13	57.39	0.1885	7.37	0.115	0.069	0.353
14	44.91	0.2040	7.05	0.090	0.079	0.337
15	33.10	0.2320	6.73	0.066	0.093	0.317
16	22.30	0.2740	6.33	0.045	0.111	0.299
17	21.15	0.3270	5.98	0.042	0.129	0.276
18	17.78	0.3805	5.52	0.036	0.179	0.253
19	14.72	0.5265	5.06	0.029		0.248
20	6.68	0.3240	4.96	0.013		

$$\Delta x = \frac{1}{20} \text{ (Length of ship) } = 26.25 \text{ ft}$$

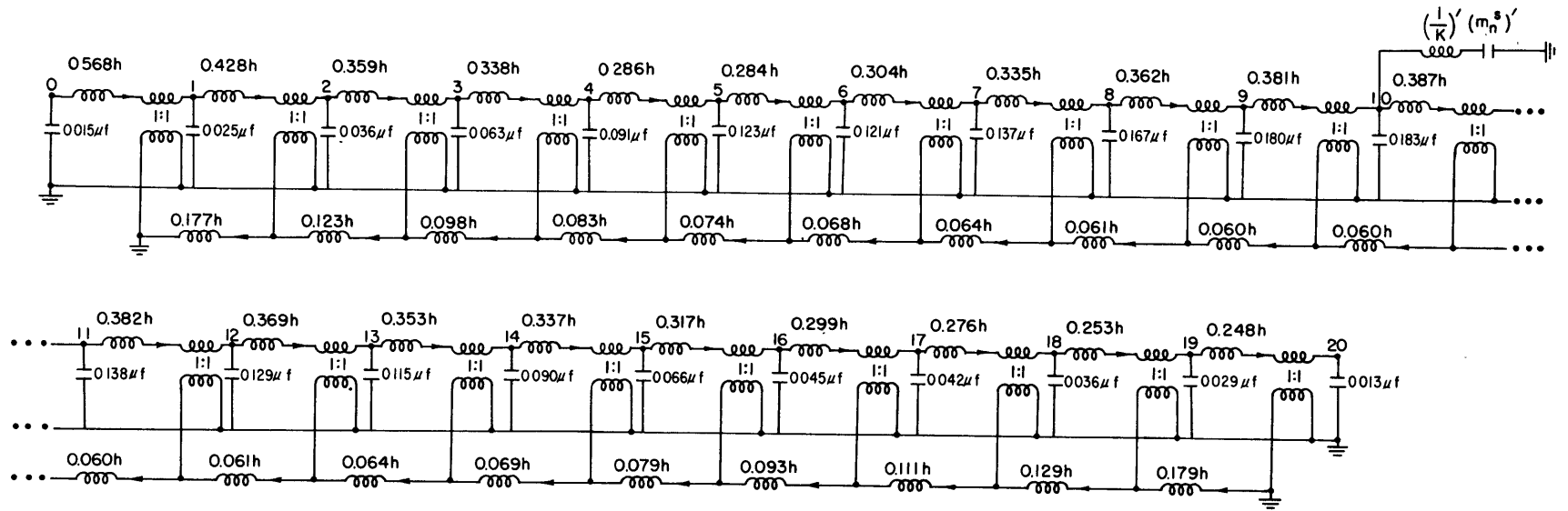


Figure 14 – Analog of 20-Section Nonuniform GOPHER MARINER Beam with Attached Sprung Mass with Bending and Shearing Flexibility

For 10 percent sprung mass  $(m_n^s)' = 0.0183 \mu f$ ;  $\left(\frac{1}{K}\right)' = 9.099h$ ; for 50 percent sprung mass  $(m_n^s)' = 0.0915 \mu f$ ;  $\left(\frac{1}{K}\right)' = 1.82h$ .

Analog is for light loading, vertical vibration condition.

## APPENDIX F

### GRAPHICAL DETERMINATION OF ADDED MODE FREQUENCY OF NONUNIFORM BEAM

Examination of Figure 13 shows that a reasonably accurate determination of  $f^t$  can be made by the following method.

1. Calculate  $f_3^t$  and  $f_4^t$  on a digital computer such as the UNIVAC and construct vertical asymptotes through these points. (It is assumed that  $f_3^t$  and  $f_4^t$  lie on opposite sides of  $f_0$ .)

2. Measure  $f_3^a$  and  $f_4^a$  on the network analyzer and construct vertical asymptotes through these points.

3. Calculate values  $\epsilon_1$  at the resonances adjacent to  $f_0$ .

4. By use of the network analyzer obtain the data necessary to plot Curve  $B$ , the TMB network analyzer solution for the beam alone.

5. Draw Curve  $A$ , the UNIVAC solution for the beam alone, knowing the values of  $\epsilon_1$  at the resonances adjacent to  $f_0$  and assuming the value  $y_p/F_p$  at any point on Curve  $A$  is displaced from the same value on Curve  $B$  by an error which is directly proportional to the frequency.

6. Mark the known value of  $f_0$  on the  $f$ -axis, Figure 13.

7. Measure  $f^a$  on the network analyzer.

8. Draw a straight line from  $(f_0, 0)$  through  $\left(f^a, \frac{y_p}{F_p}\right)$  on Curve  $B$  and extend this line to the point of intersection with Curve  $A$ . The abscissa of this point of intersection is an approximation of  $f^t$ . (For greater accuracy use the curve of Equation [1] instead of a straight line.)

## REFERENCES

1. McGoldrick, R.T., et al., "Hull Vibration Investigation on SS GOPHER MARINER," The Society of Naval Architects and Marine Engineers, Transactions, Vol. 63 (1955).
2. McGoldrick, R.T., "Calculations for Hull Vibration of the SS GOPHER MARINER and Comparison with Experimental Results," David Taylor Model Basin Report 1022 (May 1956).
3. Leibowitz, R.C., "Modes of Vibration of Rudder of USS ALBACORE (AGSS 569)," David Taylor Model Basin Report C-952 (in preparation).
4. Kennard, E.H., "Forced Vibrations of Beams and the Effect of Sprung Masses," David Taylor Model Basin Report 955 (Jul 1955).
5. Kapiloff, E., "Calculation of Normal Modes and Natural Frequencies of Ship Hulls by Means of the Electrical Analog," David Taylor Model Basin Report 742 (Jul 1954).
6. Den Hartog, J.P., "Mechanical Vibrations," Third Edition, McGraw-Hill Book Co., Inc. New York (1947).
7. Lord Rayleigh, "Theory of Sound," Vol. I, Second Edition Revised and Enlarged, Dover Publications, New York (1945).
8. Ormondroyd, J., et al., "Dynamics of a Ship Structure," Third Progress Report for the Period 31 Mar 1948 to 1 Mar 1949, Engineering Research Institute, University of Michigan, Ann Arbor, Michigan.
9. Timoshenko, S., "Vibration Problems in Engineering," Second Edition, D. Van Nostrand Co., New York (1937).

## INITIAL DISTRIBUTION

Copies		Copies	
15	CHBUSHIPS, Library (Code 312)	10	ASTIA
	5 Tech Library		
	1 Tech Asst to Chief (Code 106)		
	1 Naval Arch Planning (Code 320 E)		
	1 Applied Science (Code 370)		
	2 Noise & Vibration (Code 375)		
	1 Prelim Design (Code 420)		
	1 Ship Protection (Code 423)		
	1 Machinery Design Br (Code 430)		
	1 Mech, Sci, & Perf (Code 436)		
	1 Hull Des (Code 440)		
	1 Sci & Res (Code 442)		
2	CHBUORD, Re		
2	CHONR		
	1 Phys Sci Div (Code 420)		
	1 Math Sci Div (Code 430)		
2	DIR, USNRL, Shock & Vibration Sec		
1	CDR, USNOL		
2	NAVSHIPYD NYK, Matls Lab, Vibra Sec		
2	NAVSHIPYD PUG, Vibra Sec		
2	NAVSHIPYD PHILA, Scientific Sec		
2	NAVSHIPYD SFRAN, Vibra Sec		
1	NAVSHIPYD BSN		
1	NAVSHIPYD NORVA		
1	NAVSHIPYD PEARL		
1	NAVSHIPYD LBEACH		
1	NAVSHIPYD CHASN		
1	NAVSHIPYD PTSMH		
1	NAVSHIPYD MARE		
1	Admin, U.S. Maritime Admin		
1	COMDT, U.S Coast Guard		
1	Dir, Natl BuStand, Natl Appl Math Lab		
1	Prof. J. Ormondroyd, Dept of Engin Mech, Univ of Michigan, Ann Arbor, Mich.		
1	BSRA		









**David Taylor Model Basin. Report 1215.**  
NATURAL MODES AND FREQUENCIES OF VERTICAL VIBRATION OF A BEAM WITH AN ATTACHED SPRUNG MASS, by Ralph C. Leibowitz. September 1958. v, 39p. tables, diagrs., graphs, refs.  
UNCLASSIFIED

A study is made of the vibration characteristics of a beam with an attached sprung mass in order to explore the possibility of a more adequate representation of a ship hull as a mass-elastic system subject to vibration. Analytical and electrical-analog methods are devised to determine the natural frequencies and mode shapes of a beam-sprung-mass system. These methods are shown to give results that are reasonably accurate.

1. Beams - Vibration - Theory
  2. Beams - Vibration - Mathematical analysis
  3. Ship hulls - Vibration - Mathematical analysis
- I. Leibowitz, Ralph C.  
II. NS 712-100

**David Taylor Model Basin. Report 1215.**  
NATURAL MODES AND FREQUENCIES OF VERTICAL VIBRATION OF A BEAM WITH AN ATTACHED SPRUNG MASS, by Ralph C. Leibowitz. September 1958. v, 39p. tables, diagrs., graphs, refs.  
UNCLASSIFIED

A study is made of the vibration characteristics of a beam with an attached sprung mass in order to explore the possibility of a more adequate representation of a ship hull as a mass-elastic system subject to vibration. Analytical and electrical-analog methods are devised to determine the natural frequencies and mode shapes of a beam-sprung-mass system. These methods are shown to give results that are reasonably accurate.

1. Beams - Vibration - Theory
  2. Beams - Vibration - Mathematical analysis
  3. Ship hulls - Vibration - Mathematical analysis
- I. Leibowitz, Ralph C.  
II. NS 712-100

**David Taylor Model Basin. Report 1215.**  
NATURAL MODES AND FREQUENCIES OF VERTICAL VIBRATION OF A BEAM WITH AN ATTACHED SPRUNG MASS, by Ralph C. Leibowitz. September 1958. v, 39p. tables, diagrs., graphs, refs.  
UNCLASSIFIED

A study is made of the vibration characteristics of a beam with an attached sprung mass in order to explore the possibility of a more adequate representation of a ship hull as a mass-elastic system subject to vibration. Analytical and electrical-analog methods are devised to determine the natural frequencies and mode shapes of a beam-sprung-mass system. These methods are shown to give results that are reasonably accurate.

1. Beams - Vibration - Theory
  2. Beams - Vibration - Mathematical analysis
  3. Ship hulls - Vibration - Mathematical analysis
- I. Leibowitz, Ralph C.  
II. NS 712-100

**David Taylor Model Basin. Report 1215.**  
NATURAL MODES AND FREQUENCIES OF VERTICAL VIBRATION OF A BEAM WITH AN ATTACHED SPRUNG MASS, by Ralph C. Leibowitz. September 1958. v, 39p. tables, diagrs., graphs, refs.  
UNCLASSIFIED

A study is made of the vibration characteristics of a beam with an attached sprung mass in order to explore the possibility of a more adequate representation of a ship hull as a mass-elastic system subject to vibration. Analytical and electrical-analog methods are devised to determine the natural frequencies and mode shapes of a beam-sprung-mass system. These methods are shown to give results that are reasonably accurate.

1. Beams - Vibration - Theory
  2. Beams - Vibration - Mathematical analysis
  3. Ship hulls - Vibration - Mathematical analysis
- I. Leibowitz, Ralph C.  
II. NS 712-100



**David Taylor Model Basin. Report 1215.**

**NATURAL MODES AND FREQUENCIES OF VERTICAL VIBRATION OF A BEAM WITH AN ATTACHED SPRUNG MASS,** by Ralph C. Leibowitz. September 1958. v, 39p. tables, diagrs., graphs, refs.  
UNCLASSIFIED

A study is made of the vibration characteristics of a beam with an attached sprung mass in order to explore the possibility of a more adequate representation of a ship hull as a mass-elastic system subject to vibration. Analytical and electrical-analog methods are devised to determine the natural frequencies and mode shapes of a beam-sprung-mass system. These methods are shown to give results that are reasonably accurate.

1. Beams -- Vibration -- Theory
  2. Beams -- Vibration -- Mathematical analysis
  3. Ship hulls -- Vibration -- Mathematical analysis
- I. Leibowitz, Ralph C.  
II. NS712-100

**David Taylor Model Basin. Report 1215.**  
**NATURAL MODES AND FREQUENCIES OF VERTICAL VIBRATION OF A BEAM WITH AN ATTACHED SPRUNG MASS,** by Ralph C. Leibowitz. September 1958. v, 39p. tables, diagrs., graphs, refs.  
UNCLASSIFIED

A study is made of the vibration characteristics of a beam with an attached sprung mass in order to explore the possibility of a more adequate representation of a ship hull as a mass-elastic system subject to vibration. Analytical and electrical-analog methods are devised to determine the natural frequencies and mode shapes of a beam-sprung-mass system. These methods are shown to give results that are reasonably accurate.

1. Beams -- Vibration -- Theory
  2. Beams -- Vibration -- Mathematical analysis
  3. Ship hulls -- Vibration -- Mathematical analysis
- I. Leibowitz, Ralph C.  
II. NS712-100

**David Taylor Model Basin. Report 1215.**

**NATURAL MODES AND FREQUENCIES OF VERTICAL VIBRATION OF A BEAM WITH AN ATTACHED SPRUNG MASS,** by Ralph C. Leibowitz. September 1958. v, 39p. tables, diagrs., graphs, refs.  
UNCLASSIFIED

A study is made of the vibration characteristics of a beam with an attached sprung mass in order to explore the possibility of a more adequate representation of a ship hull as a mass-elastic system subject to vibration. Analytical and electrical-analog methods are devised to determine the natural frequencies and mode shapes of a beam-sprung-mass system. These methods are shown to give results that are reasonably accurate.

1. Beams -- Vibration -- Theory
  2. Beams -- Vibration -- Mathematical analysis
  3. Ship hulls -- Vibration -- Mathematical analysis
- I. Leibowitz, Ralph C.  
II. NS712-100

**David Taylor Model Basin. Report 1215.**  
**NATURAL MODES AND FREQUENCIES OF VERTICAL VIBRATION OF A BEAM WITH AN ATTACHED SPRUNG MASS,** by Ralph C. Leibowitz. September 1958. v, 39p. tables, diagrs., graphs, refs.  
UNCLASSIFIED

A study is made of the vibration characteristics of a beam with an attached sprung mass in order to explore the possibility of a more adequate representation of a ship hull as a mass-elastic system subject to vibration. Analytical and electrical-analog methods are devised to determine the natural frequencies and mode shapes of a beam-sprung-mass system. These methods are shown to give results that are reasonably accurate.

1. Beams -- Vibration -- Theory
  2. Beams -- Vibration -- Mathematical analysis
  3. Ship hulls -- Vibration -- Mathematical analysis
- I. Leibowitz, Ralph C.  
II. NS712-100



MIT LIBRARIES

DUPL



3 9080 02754 2833

MAR 29 1977